

1 **Human telomere length is chromosome specific and conserved across**
2 **individuals**

3

4 Kayarash Karimian^{1,2}, Aljona Groot³, Vienna Huso^{1,2}, Ramin Kahidi⁴, Kar-Tong Tan^{5,6,7},
5 Samantha Sholes^{1,2,8}, Rebecca Keener⁹, John F. McDyer¹⁰, Jonathan K. Alder¹⁰, Heng
6 Li^{11,12}, Andreas Rechtsteiner³, Carol W. Greider^{1,3,*}

7

8 ¹Department of Molecular Biology and Genetics, Johns Hopkins University School of
9 Medicine, Baltimore, MD, 21205, USA

10

11 ²Biochemistry, Cellular and Molecular Biology Graduate Program, Johns Hopkins
12 University School of Medicine, Baltimore, MD, 21205, USA

13

14 ³Department of Molecular Cell and Developmental Biology, University of California,
15 Santa Cruz,

16

17 ⁴University of Calgary, Calgary, AB, Canada

18 ⁵Harvard Medical School, Department of Genetics, Boston, MA

19 ⁶Department of Medical Oncology, Dana-Farber Cancer Institute, Boston, MA

20 ⁷Broad Institute, Cancer Program, Cambridge, MA,

21 ⁸Present address Merck & Co., 770 Sumneytown Pike, West Point, PA 19486

22 ⁹Department of Biomedical Engineering, Johns Hopkins University,

23 ¹⁰Pulmonary, Allergy, Critical Care, and Sleep Medicine Division, Department of
24 Medicine, University of Pittsburgh

25 ¹¹Dana-Farber Cancer Institute, Department of Data Sciences, Boston, MA,

26 ¹²Harvard Medical School, Department of Biomedical Informatics, Boston, MA

27 *Corresponding Author

28 Carol W Greider, PhD

29 Department of Molecular, Cell & Developmental Biology

30 University of California, Santa Cruz

31 1156 High Street

32 Santa Cruz, CA 95064

33 E-mail: cgreider@ucsc.edu

34

35

36

37

38

39

40

41

42 **Abstract**

43 Short telomeres cause age-related disease and long telomeres predispose to cancer;
44 however, the mechanisms regulating telomere length are unclear. To probe these
45 mechanisms, we developed a nanopore sequencing method, Telomere Profiling, that is
46 easy to implement, precise, and cost effective with broad applications in research and
47 the clinic. We sequenced telomeres from individuals with short telomere syndromes and
48 found similar telomere lengths to the clinical FlowFISH assay. We mapped telomere
49 reads to specific chromosome end and identified both chromosome end-specific and
50 haplotype-specific telomere length distributions. In the T2T HG002 genome, where the
51 average telomere length is 5kb, we found a remarkable 6kb difference in lengths
52 between some telomeres. Further, we found that specific chromosome ends were
53 consistently shorter or longer than the average length across 147 individuals. The
54 presence of conserved chromosome end-specific telomere lengths suggests there are
55 new paradigms in telomere biology that are yet to be explored. Understanding the
56 mechanisms regulating length will allow deeper insights into telomere biology that can
57 lead to new approaches to disease.

58

59 **Introduction**

60 Human health is profoundly affected by telomere length, yet the detailed mechanism of
61 length regulation is poorly understood. Telomere length is maintained as an equilibrium
62 distribution with constant shortening at each round of DNA replication, which is
63 counterbalanced by *de novo* addition of new telomere repeats by the enzyme
64 telomerase¹. Failure to maintain the length distribution leads to inherited Short

65 Telomere Syndromes and age-related degenerative disease such pulmonary fibrosis,
66 immunodeficiency, and bone marrow failure ². Conversely long telomeres predispose
67 people to cancer ³, and a cluster of mutations that increases telomerase activity is one
68 of the most common mutational signatures in cancer ^{4,5}.

69

70 Precisely how telomerase action maintains a length equilibrium is of great interest. The
71 prevailing 'protein counting' model for length maintenance ^{6,7} proposes that proteins that
72 bind telomeric TTAGGG repeats negatively regulate telomere elongation in *cis*. This is
73 supported by evidence that telomerase stochastically elongates short telomeres more
74 frequently than long telomeres ⁸. Together these studies propose that the length
75 equilibrium is maintained by telomerase lengthening short telomeres to precisely
76 counterbalance shortening of all telomeres. An implication of this model is that all
77 telomeres will be regulated around a similar mean length distribution.

78

79 Methods for measuring telomere length have had significant influence on length
80 regulation models. Southern blotting with a telomere repeat probe was first established
81 to measure the length of all telomeres in a population of cells and revealed a
82 heterogeneous distribution of lengths ^{9 10}. The distribution is difficult to quantitate, and
83 absolute lengths differ significantly between labs ¹¹. The protein counting model was
84 based on data from Southern blots which explains the focus on the regulation of the
85 distribution of lengths across all telomeres ¹²⁻¹⁴. The clinical FlowFISH assay ¹⁵ used for
86 diagnosis of telomere diseases ¹⁶⁻¹⁸ is normalized to the median length of telomeres on
87 a Southern blot. The fact that this method is robust and accurately identifies telomere

88 mediated disease may imply to some that the global telomere length average is the
89 biologically relevant measurement, when in fact it might not be.

90

91 Other methods such as qFISH allows measurement of individual telomeres by *in situ*
92 hybridization to a fluorescent probe in a metaphase spread ¹⁹. qFISH experiments have
93 suggested that telomeres on all chromosome arms are not globally regulated around a
94 common length distribution ²⁰⁻²², however this data is not yet reconciled with the
95 prevailing protein counting model of length regulation. FlowFISH and qFISH are not
96 accessible to researchers outside specialized telomere biology labs, highlighting the
97 need for a reproducible, accurate, and accessible tool for telomere length
98 measurements. Here we describe nanopore Telomere Profiling, which measures the
99 length of each individual telomere in the cell at nucleotide resolution. Using this
100 technique, we establish that indeed individual telomeres on specific chromosome ends
101 are maintained around their own unique length distributions, and the length distributions
102 can differ by more than 6kb. Telomere profiling represents a paradigm shift in telomere
103 analysis and will enable exploration of entirely new areas of telomere biology.

104

105

106 **Results**

107 To determine whether human telomeres are maintained around a common length
108 distribution across all chromosome ends or if specific chromosome ends maintain their
109 own unique length distributions, we developed the Telomere Profiling method to
110 physically enrich telomeres and sequence them using Oxford Nanopore Technology

111 (ONT) MinION for long read sequencing. We ligated the telomeric ends with a
112 biotinylated oligonucleotide (TeloTag) that contains a multiplexing barcode and
113 restriction enzyme sites. Following ligation, we pulled down the tagged telomeres with
114 streptavidin beads and released them by restriction enzyme digestion prior to
115 sequencing (Fig. 1a). To assess the enrichment efficiency, we prepared libraries from
116 both telomere enriched and non-enriched samples and sequenced them on an ONT
117 MinION. Enrichment recovered ~17% of total telomere input (Extended Data Fig. 1. b,
118 c), and resulted in a ~3400-fold increase in sequenced telomeres (Extended Data
119 Fig.1d and methods). We routinely multiplexed samples and generated ~50,000
120 telomere reads per flow cell with an average fragment length (subtelomere + telomere)
121 of ~20kb. The cost per sample when multiplexing was approximately \$80-140 (see
122 methods).

123

124 **Bioinformatic analysis of telomere length**

125 We developed a bioinformatic pipeline to determine both “bulk length” (all telomeres) as
126 well as chromosome end-specific telomere length. We used ONT Guppy for nucleotide
127 base calling and filtered for reads containing telomere repeats (Methods). We initially
128 determined telomere length using a method we used in yeast²³ that has been
129 previously used in human cells²⁴⁻²⁶. Reads are first mapped to a reference genome
130 with a defined telomere/subtelomere boundary and telomere length is defined as the
131 number of base pairs from the boundary to the end of the read (Methods). However,
132 we found heterogeneity in subtelomere sequences among individuals, where
133 sometimes the subtelomere was slightly longer or shorter than in the reference genome

134 which caused overcalling or under calling of telomere lengths (Extended Data Fig. 2).
135 To overcome this, we developed TeloNP, an algorithm to define the subtelomere
136 boundary and measure telomere length directly from the nanopore sequencing reads
137 while taking systematic nanopore basecalling errors ²⁷ into account. TeloNP scans from
138 the end of the read and defines the subtelomere boundary where it finds a sustained
139 deviation from the expected telomeric sequence content (Fig. 1b and Extended Data
140 Fig. 3) (see Methods). Telomere length was defined as the base pairs from the TeloTag
141 to the subtelomere boundary identified by TeloNP in the telomere read.

142

143 To examine whether telomere length determined by TeloNP after Guppy base calling
144 accurately represents the true length of the telomere repeats, we examined the
145 electrical current signals from the flow cells. We developed TeloPeakCounter to count
146 the repeated current peaks corresponding to (TTAGGG)_n in telomere sequences and
147 estimate telomere length (Extended Data Fig. 4a, b) (see methods). We found telomere
148 length determined by TeloNP after Guppy base calling was in good agreement with
149 length determined by TeloPeakCounter. We therefore adopted Guppy base calling for
150 our analyses. We note the new ONT Dorado base caller (version 0.3.1) overestimated
151 telomere length for G strand reads compared with both TeloPeakCounter and Guppy
152 (Extended Data Fig. 4 c, d).

153

154 **Nanopore Telomere Profiling accurately and reproducibly reports telomere length**

155 We performed Telomere Profiling by sequencing DNA from Blood or PBMCs (see
156 methods) of 132 people ranging from 0 years to 91 years of age (Fig. 1d) and found

157 agreement with telomere lengths on a Southern blot (Fig. 1c). To test reproducibility, we
158 measured telomere length of DNA from one individual on the same flow cell (intra-
159 assay) (Fig. 1e and Extended Data Fig. 1e) (coefficient of variation, CV 1.3%) or on
160 different flow cells (inter-assay) Fig. 1f and Extended Data Fig. 1f (CV 2.4%). This low
161 variability compares well with FlowFISH that has an inter-assay CV of 2.2%, and
162 considerably outperformed the frequently used qPCR assay that has an inter-assay CV
163 of 25.0%¹⁷. In addition, we tested inter-lab variability by measuring telomere length of
164 seven samples where the same DNA was enriched and sequenced by two different
165 people in two different labs (Johns Hopkins and UCSC) and found highly reproducible
166 results (mean difference of 104.7 bp with SEM of +/- 34 bp) (Fig. 1g). To determine
167 whether any fragment length bias of nanopore sequencing could skew telomere length
168 determination, we compared restriction enzyme cutting with a combination of *BamHI*
169 and *EcoRI* which generates fragments ~9 kb, or with *AsiSI* and *PvuI*, which generate
170 fragments ~25 kb. We found similar telomere lengths in these two samples (6,127 bp vs
171 6,188 bp) (Extended Data Fig. 5a, b) indicating fragment length in these size ranges did
172 not have detectable bias on telomere length determination.

173

174 **Telomere profiling determines telomere shortening with age at nucleotide** 175 **resolution**

176 Telomere length is known to shorten with age^{17,28-31}, however previous methods could
177 not measure telomere length at nucleotide resolution. To test the dynamic range of
178 Telomere Profiling, we first applied nanopore Telomere Profiling to DNA samples of 11
179 individuals from 0-84 years of age and ordered the samples based on decreasing

180 telomere length (Fig. 2a). We then did a Southern blot on the same DNA and found
181 Telomere Profiling predicted the relative order of telomere lengths and captured the
182 wide dynamic range of the Southern blot (Fig. 2a and b). Southern blotting does not
183 measure the shortest telomeres because telomere repeats are required for probe
184 hybridization on a Southern. We plotted the 1st, 10th and 50th percentile of telomere
185 length as determined by Telomere Profiling and observed a decrease of the 50th and
186 10th percentile as the mean length shortened. However, the 1st percentile telomere
187 length did not decrease suggesting there is a threshold length in PBMC's of below
188 which telomeres cannot be maintained (Fig. 2c).

189
190 To directly compare nanopore Telomere Profiling to FlowFISH, we conducted nanopore
191 Telomere Profiling on whole blood and PBMCs (see methods) of 132 donors ranging
192 from 0 to 90 years of age (Fig. 2d). Using the mean telomere length for each individual,
193 we defined 90th, 50th and 10th intervals of telomere length at each age using the same
194 statistical methods used for FlowFISH¹⁷. While the shapes of the curves are very
195 similar between Telomere Profiling and FlowFISH, the absolute lengths of the telomeres
196 are longer for FlowFISH. Nanopore Telomere Profiling of cord blood showed a telomere
197 length distribution with a mean of 7,986 +/- 245 bp (Fig. 2d) across 18 samples. This is
198 shorter than the average cord blood telomere length for FlowFISH and with less
199 variance (Fig. 2e)¹⁷. Average cord blood telomere length estimates measured by
200 FlowFISH vary from ~18kb³² to ~9kb³³ to ~11 kb¹⁷. FlowFISH fluorescence signal is
201 normalized to Southern blots, which includes some subtelomeric sequences and this
202 may account for the longer telomere lengths of FlowFISH. Furthermore, Southern blot

203 estimated telomere lengths are known to vary between laboratories ¹¹. In contrast,
204 nanopore Telomere Profiling offers a precise readout in base pairs that can be directly
205 compared between laboratories.

206

207 To compare our method directly to FlowFISH, we sequenced 5µg of archived DNA from
208 blinded samples of individuals previously diagnosed with Idiopathic pulmonary fibrosis
209 (IPF) one of the Short Telomere Syndromes ³⁴. Telomere profiling showed that bulk
210 telomere length in most IPF samples were similar to the FlowFISH measurement (Fig.
211 2f). FlowFISH uses flow cytometry and can distinguish telomere lengths in specific cell
212 types from whole blood samples ^{35,36} and some samples have discordant lymphocyte
213 and granulocyte telomere lengths ^{17,37,38}, Nanopore Telomere Profiling will report the
214 average length from all cell types in the samples. Thus, while nanopore Telomere
215 Profiling likely can be used for diagnosing Short Telomere Syndromes in the future,
216 additional development such as isolation of specific cell types may help to capture
217 heterogeneity of clinical samples.

218

219 **Human telomeres have chromosome end-specific length and haplotype-specific** 220 **length differences**

221 To determine whether humans have chromosome end-specific telomere length, we first
222 examined telomeres from the diploid HG002 cell line for which a high-quality reference
223 genome is available ³⁹. Human subtelomeres contain many blocks of homology shared
224 between different telomeres (paralogy blocks) ^{24,40}. Simulation of long read data from
225 CHM13 references genome showed that *minimap2* ^{41,42} can assign simulated reads to

226 the correct telomere with high accuracy using 10kb of subtelomere sequence²⁷. We
227 isolated DNA from HG002 cell line, sequenced the telomeres and mapped reads with
228 an average total length of 16.4 kb (4.6 kb telomere repeats and 11.8 kb sub-telomeric
229 sequence, on average) to the HG002 reference genome using *minimap2* using a
230 customized filtering pipeline (methods). Seventy-seven chromosome ends passed our
231 quality filters, and we found 66 ends had significant differences in length distribution
232 from the grand mean (Fig. 3. a, b). In addition to chromosome end-specific lengths, we
233 also found that some telomeres showed significant differences between the maternal
234 and paternal haplotypes. In some cases, remarkably, there was more than 6kb
235 difference in mean length, for example for chromosome 1p Maternal (1pM) and 1p
236 Paternal (1pP). Thus, like in yeast²³, humans have chromosome end-specific telomere
237 length distributions.

238

239 **Chromosome specific telomere lengths are conserved across individuals.**

240 To determine whether chromosome end-specific differences were conserved across a
241 broad population, we used *minimap2* to map ~920000 telomere reads from 147
242 individuals to the subtelomere sequences from the recently released pangenome
243 containing 47 high quality T2T assemblies⁴³ and filtered for reads with >1kb of
244 alignment, which resulted in ~647,000 reads (see methods). We removed the
245 acrocentric and X Y chromosome ends because the high rate of meiotic recombination
246 between these ends across a population would not allow them to map uniquely⁴⁴.

247

248 *Minimap2* map quality score (mapq) is not optimized for mapping to the multiple
249 genomes present in the pangenome as most reads have multiple near identical
250 alignments and thus get low mapq. To establish if reads reproducibly mapped to the
251 same subtelomere, we compared the pangenome alignment of reads to their alignment
252 in three different high quality haploid reference T2T genomes CHM13, HG002 maternal
253 and HG002 paternal. Of the ~647,000 reads that aligned to the pangenome ~350,000
254 mapped to the T2T references with a mapq of 60. We compared the fraction of reads
255 that were mapped to a given chromosome end in the pangenome (column) to where
256 they mapped in the respective T2T haploid genome (rows) in a matrix heatmap (Fig. 4
257 a, b, c). The diagonal indicates the fraction of reads mapping to a chromosome in the
258 pangenome that map to the same chromosome end in the respective haploid genomes.
259 87% of the filtered reads mapped to the same chromosome end in the pangenome and
260 CHM13, 90% in the pangenome and HG002 maternal and 88% in the pangenome and
261 HG002 paternal. We also quantified the percent of reads that mapped to the same
262 chromosome end in the pangenome and all three haploid reference genomes (Fig. 4d
263 and Extended Data Fig. 5 a, b, c). For 33 of the 39 chromosomes ends, 100-60% of the
264 reads mapping to a given chromosome end in the pangenome mapped to the same end
265 and all three haploid genomes. Six chromosome ends had between 10-20% of reads
266 map to the same chromosome end in the pangenome and all three haploid genomes.
267 When we added back the acrocentric chromosomes, we found 0 reads mapped back to
268 the same chromosome end in all three references (Extended Data Fig 5d), as expected
269 for reads that map to several different chromosome ends across a population. Together

270 this data suggests that the reads we found mapping to a certain pangenome
271 chromosome map with high confidence.

272

273 To compare the telomere length of each chromosome end across the aging population,
274 we established the relative mean telomere length. For the ~640000 reads that mapped
275 to the pangenome, we calculated the grand mean telomere length for a given individual
276 and subtracted it from the chromosome specific mean telomere length for each
277 chromosome end for a given individual. Zero indicates no difference between the
278 specific chromosome end mean telomere length and the individual's grand mean
279 telomere length (Fig 4e). We ranked the chromosome ends by their relative telomere
280 lengths and found that 17p, 20q and 12p tended to be the shortest telomeres in the
281 population while 4q, 12q and 3p tended to be the longest (Fig. 4e). Thus, while
282 haplotype specific differences in telomere length are seen in a single individual (Fig.
283 3a), across a population, on average, certain chromosome ends are more likely to be
284 shorter while others are more likely to be longer than the grand mean. Remarkably,
285 previous work using qFISH to measure telomere length on metaphase spreads in 10
286 individuals also found 17p, 20q and 12p among the top 4 shortest and 4q, 12q and 3p
287 among the top 8 longest ends ²¹ strengthening the conclusion that some chromosome
288 ends are reproducibly shorter or longer than the grand mean.

289

290 To determine whether chromosome end-specific telomere lengths are present at birth,
291 we mapped the reads from cord blood to the pangenome and calculated the relative
292 mean telomere lengths as described above (Fig. 4f). While we had fewer cord blood

293 samples, and therefore fewer chromosome ends met our quality filters, we found again
294 that 17p, 20q and 12p were shorter while 4q, 12q and 3p were longer than the grand
295 mean. This supports previous work ⁴⁵ that suggested that telomere length at birth is
296 maintained with age.

297

298

299 **Discussion**

300 A fundamental understanding of the mechanisms that regulate telomere length is
301 essential to develop future disease treatments. When the telomere length distribution
302 shifts to shorter lengths, some telomeres become critically short, initiating senescence,
303 ⁴⁶⁻⁴⁹ and can cause age-related degenerative disease in humans ¹⁸. Inherited mutations
304 that shift to a longer equilibrium predispose people to cancer ^{3,50} and the most frequent
305 somatic mutations in cancer increase telomerase levels and lengthen telomeres ^{4,5}.
306 Nanopore Telomere Profiling will enable the dissection of how individual telomere
307 lengths on specific chromosomes are maintained and may play a role triggering
308 senescence, and ultimately in disease.

309

310 **Chromosome end-specific telomere length equilibria imply new regulatory**

311 **mechanisms**

312 The predominant protein counting model for telomere length maintenance proposes that
313 telomere proteins that bind TTAGGG repeats repress the elongation of a given telomere
314 in *cis* ^{6,51} and longer telomeres have more repression, allowing shorter telomeres to be
315 preferentially elongated ⁸. This model represents a robust way to maintain a length
316 equilibrium ⁵². However, since all telomeres have the same TTAGGG repeats, the

317 model predicts that all telomeres would be regulated around a shared equilibrium
318 length. The demonstration of end-specific lengths indicates that other, yet unknown
319 factors, can play a key role modifying the set point for each unique telomere length
320 distribution.

321
322 In yeast that lack telomerase, all chromosome end-specific length distributions
323 shortened at similar rates ²³, suggesting telomere elongation, not shortening, is the
324 major influence on chromosome specific length. Telomere elongation is the sum of the
325 frequency of elongation of any given end (telomerase recruitment) and number of
326 repeats added per elongation event (telomerase processivity). When the sum of these
327 events, on average, equals the rates of telomere shortening, the equilibrium point is set.
328 However, given end-specific length distributions, it is clear that this simple view does not
329 represent the full complexity of the system. There must be factors at specific
330 chromosome ends that regulate telomerase recruitment, processivity, or both, to
331 establish end specific lengths. In addition, stochastic shortening such as telomere rapid
332 deletion ⁵³ or replication fork collapse ^{54,55} may play yet unknown roles in establishing
333 telomere length equilibrium.

334

335 **Mechanisms that may influence end specific telomere length**

336 Subtelomeric sequences are obvious candidates to regulate end-specific telomere
337 lengths. In yeast, subtelomere DNA binding proteins can affect telomere length ⁵⁶,
338 although the mechanism is not yet understood. The subtelomeric TAR1 element ⁵⁷
339 present in paralogy block 23 ^{26,40} was proposed to regulate telomere length, possibly

340 through binding CTCF and regulating expression of the lncRNA, TERRA⁵⁸⁻⁶⁰. Previous
341 studies suggested that the absence of TAR1 may correlate with shorter telomeres²⁶.
342 However, we did not find a direct relationship of the shortest telomere with those ends
343 described by Dubocanin *et. al.* that lack TAR1 (8q,13p,14p, 17p, 21p, 22p Xp) in our
344 data set. Future comprehensive analysis of the subtelomere sequences adjacent to long
345 and short telomeres will lead to new testable models for establishment of telomere
346 length equilibria.

347

348 Epigenetic modifications of DNA or histones may influence telomere length⁶¹. Human
349 and mouse subtelomeric regions are known to be methylated at CpG sites⁶² and
350 experiments in mice suggest that loss of DNA methyltransferases results in shorter
351 telomeres⁶³. Sequences in the subtelomere could recruit chromatin modifying enzymes
352 that might influence length regulation. Subtelomere sequences may also influence other
353 mechanisms that have been proposed to regulate telomere length including replication
354 timing and tethering to the nuclear periphery⁶⁴. The availability of nanopore Telomere
355 Profiling will allow exploration of the role of these factors in establishing telomere length
356 equilibria.

357

358 **Chromosome end-specific length differences are present at birth and maintained**
359 **as telomeres shorten with age**

360 Telomere length is inherited from parent to child. Evidence of this comes from the
361 genetic anticipation in Short Telomere Syndromes; short telomeres are passed down to
362 each generation, and the severity of disease increases across generations⁶⁵. Similarly,

363 in mice heterozygous for telomerase deletion, short telomeres are progressively passed
364 down across 6 generations causing progressive severity of disease⁶⁶. Twin studies
365 have also documented the inheritance of telomere length in humans⁶⁷.

366

367 Analysis of chromosome end-specific telomere lengths across 147 individuals showed
368 specific telomeres tend to be the longest or shortest, supporting a previous study using
369 qFISH on 10 individuals that identified a similar set of chromosomes as the longest and
370 shortest²¹. Cord blood also showed that 17p, 20q and 12p were among the shortest
371 and 4q, 12q and 3p were among the longest ends suggesting that telomere length
372 differences present at birth are maintained over decades. This establishment of
373 chromosome-end specific telomere length equilibria at birth⁴⁵ and maintenance of the
374 equilibria after birth leaves little room for proposed effects of life history, psychological,
375 or environmental exposures⁶⁸ on telomere length. The similarity of our data with
376 Martens *et al.* qFISH analysis is remarkable, and our method will enable future studies
377 to explore the biological significance of this finding. We did not prospectively choose our
378 samples to be representative of the diversity of the human population, but rather to span
379 a wide age range. However, future studies could be powered to examine whether
380 certain chromosome ends are consistently the shortest or longest more broadly in a
381 diverse human population.

382

383 **Implications for human disease**

384 Being able to accurately measure chromosome-end specific telomere length has
385 important implications for human disease. Nanopore Telomere Profiling determines

386 nucleotide resolution of the length distribution and can distinguish the length of specific
387 chromosome ends unlike Southern blots, qPCR, or FlowFISH assay. Telomere profiling
388 employs the accessible MinION instrument that can be used in-house in any research
389 or clinical lab, with very low start-up costs, allowing for equitable access to telomere
390 length determination methods. This method provides the opportunity to prospectively
391 develop clinical standards analogous to those for FlowFISH and may allow clinical
392 length measurements in samples other than blood. In addition, having a highly
393 reproducible assay that can be easily automated will enable experimental approaches
394 to define new regulators of telomere length. The role telomere elongation in the
395 immortalization of cancer cells has been known since 1990^{29,69,70}. Having a precise tool
396 that can be automated, will allow new approaches that may exploit telomere length
397 modulation in cancer treatment. Finally, the identification of conserved chromosome
398 end-specific telomere lengths implies that new, undiscovered biological mechanisms
399 influence telomere length. Nanopore Telomere Profiling will empower the field as a
400 whole to dissect these mechanisms, leading to new discoveries in telomere biology.

401

402 **Methods**

403 **Human subjects**

404 Peripheral blood mononuclear cells (PMBCs) were purchased from Stem Cell
405 Technologies, ZenBio Inc, and Precision for Medicine. Samples were chosen from the
406 repositories based on age to span from 0 (cord blood) to 91 years. Research consent
407 for these samples was obtained by the respective companies. Blood samples used to

408 calibrate the assay were de-identified excess samples from Johns Hopkins Hospital,
409 certified as exempt by the John Hopkins University School of Medicine IRB.
410 For the Short Telomere Syndrome analysis, all subjects provided written, informed
411 consent before enrollment in the study. Research subject were recruited from the lung
412 transplantation clinic at the University of Pittsburgh Medical Center. All patients were
413 diagnosed with idiopathic pulmonary fibrosis according to consensus guidelines of the
414 American Thoracic Society and European Respiratory Societies at the time of their
415 enrollment ⁷¹.

416

417 **Cell Lines**

418 HG002 cells were cultured in RPMI 1640 media (Gibco, Cat.11875093) supplemented
419 with 2g/L glucose 2mM L-glutamine (Glutamax, Gibco, Cat.35050061) 15% fetal bovine
420 serum (Gibco, Cat.26140079) and 1% penicillin-streptomycin (Gibco, Cat.15140122).
421 PBMCs were counted using the Luna II hemocytometer (VitaScientific,
422 Cat.LGBD10029).

423 **Telomere Southern blot analysis**

424 Genomic DNA was isolated using the Promega Wizard gDNA kit (Cat.A1120, Promega)
425 and quantified by QuBit 3.0 (Thermo Fisher) using the DNA kit (Q32853; Thermo
426 Fisher). Approximately 1 µg of genomic DNA was restricted with *Hinfl* (NEB,
427 Cat.R0155M) and *RsaI* (NEB, Cat.R0167L,) and resolved by 0.8% Tris-acetate-EDTA
428 (TAE) agarose gel electrophoresis (Invitrogen, Cat.EA0375BOX). 10 ng of a 1kB Plus
429 DNA ladder (NEB, Cat.N3200) was included as a size reference. Following denaturation

430 (0.5 M NaOH, 1.5M NaCl) and neutralization (1.5 M NaCl, 0.5 M Tris-HCL, pH 7.4) the
431 DNA was transferred in 10x SSC (3M NaCl, 0.35 M NaCitate) to a Nylon membrane
432 (GE Healthcare, Cat. RPN303B) by vacuum blotting (Boekel Scientific). The membrane
433 was UV crosslinked (Stratagene), prehybridized in Church buffer (0.5M Na₂HP0₄,
434 pH7.2, 7% SDS, 1mM EDTA, 1% BSA), and hybridized overnight at 65°C using a
435 radiolabeled telomere fragment and ladder, as previously described (Morrish and
436 Greider 2009). The membrane was washed twice with a high salt buffer (2x SSC, 0.1%
437 SDS) and twice with a low salt buffer (0.5X SSC, 0.1% SDS) at 65°C, exposed to a
438 Storage Phosphor Screen (GE Healthcare), and scanned on a Storm 825 imager (GE
439 Healthcare). The images were copied from ImageQuant TL (GE Life Sciences) to
440 Adobe PhotoShop CS6, signal was adjusted across the image using the curves filter,
441 and the image was saved as a .tif file.

442 **FlowFISH**

443 FlowFISH was performed in the Johns Hopkins Pathology Molecular Diagnostics
444 Laboratory as described in Alder et al. 2018¹⁷.

445 **Preparation of HMW DNA**

446 A modified DNA extraction protocol was used to produce high molecular weight DNA
447 based on the Lucigen/EpiCentre's MasterPure™ Complete DNA and RNA Purification
448 Kit A (Biosearch Technologies, Cat MC85200). For HG002 cell line, fresh or frozen cell
449 pellets were osmotically lysed in presence of 150mL of Nuclei Prep Buffer (NEB,
450 Cat.T3052) supplemented with 5.5 mL of Rnase A (NEB, Cat. T3018L) and 5.5 mL of
451 RNase If (NEB, Cat. M0243L) per million cells for 15 seconds and mixed by flicking.

452 For PBMC or fresh blood samples, an optional PBS wash followed by Red Blood Cell
453 lysis step was included (10 mins at RT) prior to hypotonic lysis with Nuclei Prep Buffer
454 (NEB, Cat.T3052) and Rnase digestion. Nuclei from 1 million cells were lysed with 300
455 mL of lysis buffer supplemented with 20 mL of Proteinase K (20mg/mL) (ThermoFisher,
456 Cat. 25530049). Lysates were incubated at 50 degrees C for a minimum of 24 hours
457 overnight with periodic vortexing at low speeds (minimum speed to achieve swirling of
458 the solution). 150 mL of MPC Protein Precipitation Reagent solution from the
459 Lucigen/EpiCentre's MasterPure™ Complete DNA and RNA Purification Kit A was
460 added to precipitate proteins followed by centrifugation at 2000 x g for 30 mins. DNA
461 was precipitated by adding 500 mL of cold isopropanol (100%) (Supply Store,
462 Cat.100209) and pelleted by centrifugation (2000 x g for 20 mins). DNA pellets were
463 washed 3X with 70% ethanol and hydrated in pre-warmed (37°C) Elution buffer
464 (Qiagen, 10 mM Tris-Cl, pH 8.5. Cat. 19086) and incubated on HulaMixer™ Sample
465 Mixer (Thermo Fisher Scientific, Cat. 15920D) at 37°C incubator overnight at 1rpm end
466 over end mixing.

467 **Annealing of TeloTags for duplex barcode assembly:**

468 TeloTags were prepared in 100µL reactions with 5mM of each of the 6 permutations of
469 telomere splint Extended Data Fig.1A) and 30 mM of biotinylated adapter in HiFi Taq
470 DNA Ligase Reaction Buffer (NEB, Cat. M0647S). Annealing was done by heating to 99
471 degrees and slowly decreasing the temperature 1°C /min in a Veriti™ 96-Well Thermal
472 Cycler (Applied Biosystems, Cat. 4375786). After annealing, reactions were diluted
473 1:100 in 1x Taq buffer and kept at 4°C. The sequences of the TeloTag and splint
474 adapter is listed in Extended Data Table 2)

475

476 **Telomere Tagging**

477 High molecular weight genomic DNA (gDNA) was quantified using the Qubit dsDNA BR
478 assay kit (Thermo Fisher Scientific, Cat.Q32850). A total of 40 µg of gDNA was
479 incubated with 3µl of Clal (NEB, Cat. R0197S) or AsiSI (NEB, Cat.R0630L) or Pmel
480 (NEB, Cat.R0560L), or BamHI (NEB, Cat.R0136M) for 2 hours at 37°C, with gentle
481 flicking every 20 mins. Subsequently, the enzyme was heat-inactivated at 65°C for 20
482 mins. Ligations were carried out using 4 µg of DNA per 50 µl reaction.

483 Tagging reactions were done in 50 µL volume for each reaction in a MicroAmp™ TriFlex
484 Well PCR Reaction Plate (Applied Biosystems, Cat. A32811), with 4µl/reaction of 0.3µM
485 duplex TeloTag adapter, 5µl/reaction of 10X HiFi Taq DNA Ligase Reaction Buffer
486 (NEB, Cat. M0647S), and 1µl/reaction of HiFi Taq DNA Ligase (NEB, Cat. M0647S).
487 The TeloTagging reactions were incubated for 5 mins at 65°C in a Veriti™ 96-Well
488 Thermal Cycler (Applied Biosystems™, Cat.4375786). Ligations were done through 15
489 cycles of denaturing at 65°C for 1 min, followed by annealing and ligating at 45°C for 3
490 mins with a 15% ramp down of rate between steps.

491

492 **Telomere Enrichment and Nanopore Sequencing**

493 For chromosome-specific telomere length measurements, we typically used 30-40 µg of
494 DNA per sample. A standard 3 mL tube of blood or 30 million PBMC produced ~200 ug
495 of DNA. For bulk telomere length measurements, as little as 5-10 µg of starting gDNA
496 was employed. All pipetting was performed using wide bore pipette tips to minimize
497 DNA shearing, except for addition of SPRI beads where accurate volume ratios are

498 extremely important for successful cleanups. All the Telomere Tagging reactions were
499 pooled in DNA LoBind (Eppendorf, Cat.0030108523) tube. Cleanup and removal of
500 excess TeloTag adapters was done using SPRI beads (Beckman Coulter, Cat. B23318)
501 a ratio SPRI beads to DNA of 45 μ L:100 μ L was used. The samples were incubated
502 with SPRI beads rotating end over end on a Hula mixer for 20 mins at 10rpm. SPRI
503 beads were then separated using a DynaMag™-2 Magnet (Thermo Fisher Scientific,
504 Cat. 12321D) and washed while on the magnet twice with freshly made 85% ethanol.
505 DNA was eluted using heated (65 °C) 1X rCutsmart Buffer. The volume of elution
506 volume was calculated to achieve 150 ng/ml final concentration based on input DNA
507 amount. The eluting SPRI beads were incubated for 20 mins at 65°C with gently flicking
508 every 5 mins. SPRI beads were removed using a DynaMag™-2 Magnet.
509 The gDNA recovery was quantified using the Qubit dsDNA BR assay kit. Tagged gDNA
510 was enriched using Dynabeads™ MyOne™ Streptavidin C1 (Thermo Fisher Scientific,
511 Cat. 65001). The beads were allowed to room temperature while being resuspended on
512 a HulaMixer™ Sample Mixer (Thermo Fisher Scientific) at 3 rpm for 1h. A ratio
513 streptavidin to DNA of 1 μ g:250ng was used. The beads were washed once in Binding
514 Buffer from Dynabeads™ kilobaseBINDER™ Kit and resuspended in equal volume
515 binding buffer as eluted DNA volume. The beads were then added to the gDNA sample
516 and incubated at room temp at 1 rpm on a HulaMixer™ Sample Mixer for 20 mins.
517 Reactions can be scaled up or down as needed, though the maximum volume of beads
518 + gDNA + binding buffer should not exceed 1.4 ml for a single 1.5 ml Protein LoBind
519 tube (Eppendorf, Cat. 30108442). Multiple tubes can be used and pooled at the
520 restriction enzyme digest step. After binding to streptavidin, the beads were washed

521 using the following sequence to remove background genomic DNA: 2x kilobaseBinder
522 wash buffer, 2x Elution buffer (Qiagen, 10 mM Tris-Cl, pH 8.5), 1x rCutsmart Buffer.
523 To release telomeres, the streptavidin bead-telomere complex was resuspended in 72
524 μ l of 1X rCutsmart, 3 μ l of PvuI (NEB, Cat. R3150S) PacI (NEB, Cat. R0547L) or EcoRI
525 (NEB, Cat.R0101M), and incubated at 37°C for 30 min, with periodic gentle flicking. The
526 sample was then heated at 65°C for 20 mins to release any bound telomeres. If multiple
527 tubes were used, sequential rounds of digestion can be used by adding restriction
528 enzyme to the eluted telomere solution from the first step and incubating with
529 streptavidin-telomere beads in the second tube. Recovered tagged gDNA was
530 quantified using the Qubit dsDNA HS assay kit. The expected recovery was
531 approximately 0.1-0.01% of the starting gDNA sample.

532 Enriched telomeres were carried forward into the standard Nanopore library prep
533 protocol from ONT. All reactions were prepared using Ligation Sequencing Kit V10
534 (SQK-LSK114) kits and sequenced on R9.4.1 (Oxford Nanopore Technologies, FLO-
535 MIN106D) flow cells. Libraries were eluted in 40 ml of elution buffer (Qiagen, 10 mM
536 Tris-Cl, pH 8.5) with optional 15 mins of incubation at 37°C to recover long molecules.
537 Each library was split into 3 reactions. Each reaction was sequenced on a flow cell for
538 ~18 hours before flow cell flushing/washing using flow cell wash kit (Oxford Nanopore
539 Technologies EXP-WSH004) and loading of the remaining fraction. Reads were
540 collected using MinKNOW software (5.7.5) without live basecalling.

541

542 **Cost per sample for telomere enrichment and sequencing.**

543 Library construction and nanopore sequencing cost were \$750 per library including
544 \$500 for flow cell. We used multiplexing strategies to lower the cost. For bulk telomere
545 pulldown and sequencing used 10 μ g DNA for each sample and multiplexed 10 for a
546 cost of ~\$80 each sample. For chromosome-specific telomere pulldown and
547 sequencing we started with 40 μ g DNA and multiplexed 8 samples for a cost of ~\$140
548 per sample.

549

550 **Determination of telomere/subtelomere boundary position and telomere length**

551 To determine the length of the telomere repeats, we tested two methods. One method is
552 based on determining the junction of the telomeres and subtelomeres in the respective
553 reference genome (CHM13, HG002 maternal and HG002 paternal) and the second
554 method determines the subtelomere to telomere junction in every read. For method 1, to
555 determine the junction in a reference genome, we developed a Python algorithm named
556 TeloBP (Telomere Boundary Point). TeloBP employs a rolling window approach,
557 scanning from the telomere into the chromosome, identifying the telomere-subtelomere
558 junction by detecting a discontinuity in a user defined telomeric pattern. The algorithm's
559 default telomeric pattern is a sequence where at least 50% of nucleotides are "GGG".
560 As the window moves along at six nucleotide intervals, it scores telomere similarity in
561 100-nucleotide segments. Variants of the telomere repeats known to be in the
562 subtelomere do not significantly change sequence content. The junction is defined when
563 the sequence content no longer matches a telomere like sequence content. This is
564 calculated by averaging the similarity of a sequence with a 500 bp window, marking the
565 start of a 50% deviation, then scanning until the increase in discontinuity plateaus,

566 marking the subtelomere boundary. After reads are mapped to the reference genome,
567 for each read the telomere length is determined as the number of base pairs from
568 subtelomere junction in the reference to the TeloTag. This method incorporated many
569 variant telomere repeats into the telomere that are not incorporated by identifying the
570 boundary as 4X TTAGGG (Extended Data Fig 3).

571 In the second method we determined the subtelomeres/telomeres boundary in each
572 read. We developed a version of TeloBP that considers common errors in the nanopore
573 Guppy base calling. These patterns are set by default based on findings in ²⁷,
574 “[^GGG]GGG[^AAA]AAA|TTAGG.” for G strand and “CTTCTT|CCTGG|CCC...” C
575 strands. But the patterns can be user defined as new base callers are developed. We
576 named this algorithm TeloNP (Telomere NanoPore). Both TeloBP and TeloNP are
577 available on Github (<https://github.com/GreiderLab>).

578 **Custom genome for mapping telomeres**

579 For mapping reads to the T2T genomes CHM13 and HG002 we generated custom
580 reference genomes. We first extracted the terminal 500kb of chromosome end for each
581 genome, then removed the telomere repeats (as determined by TeloBP) from the
582 reference genome to allow for maximized weighing of subtelomere information for read
583 mapping.

584

585 **Bioinformatic filtering of telomere reads**

586 Reads were first filtered for any of the following telomere patterns [“TTAGGGTTAGGG”,
587 “TTAAAATTTAAAATTTAAA”, “CCCTCCGATA”, “TGGCCTGGCCTGGCC”] based on
588 findings in previous literature ²⁷. To identify reads with a TeloTag at the end and to

589 demultiplex samples we performed a pairwise alignment of the 24bp barcodes with the
590 terminal 300bp of each read using the pairwise Alignment function in the Bio Strings
591 package of Bioconductor (doi:10.18129/B9.bioc.Biostrings , R package version 2.68.1,
592 <https://bioconductor.org/packages/Biostrings>). The alignment score cutoff was set so
593 the false discovery rate for our nanopore reads was < 1% based on random 24bp
594 barcode sequences and unused ONT barcode sequences. We used Minimap2 with the
595 -x map-ont option to map our reads to the custom genomes HG002 and CHM13⁴². We
596 only considered primary alignments that started within 1 kb of the subtelomere
597 boundary.

598

599 **Peak calling to measure telomere length with TeloPeakCounter**

600 To examine whether the Guppy (v 6.5.7) and Dorado (v 0.3.1) base caller accuracy call
601 the telomere length in correctly, we developed an algorithm, TeloPeakCounter, to count
602 repeated peaks, or waves, in the electrical signal data measured by the nanopore
603 device. These distinct repeated waves found in the telomere region of reads correspond
604 to the TTAGGG telomere repeat sequences. TeloPeakCounter analyzes and counts
605 these distinctive, periodic wave patterns in the electric signal data, and enables a direct
606 measurement of telomere length. Assuming each wave represents a 6-nucleotide
607 telomere repeat, we can compute estimated telomere lengths for a read. The code
608 for TeloNP and TeloPeakCounter is available at GitHub (<https://github.com/GreiderLab>)

609

610 **Mapping HG002 subtelomere to maternal and paternal alleles**

611 For the diploid HG002 genome some maternal and paternal subtelomere sequences
612 are very similar and correct assignment of reads becomes difficult. We developed a
613 two-step mapping procedure for mapping HG002 reads. In the first step, reads are
614 mapped to the HG002 diploid genome. Mapq mapping confidence scores are set low for
615 these mappings, as the mapper can have difficulty deciding between very similar
616 maternal and paternal subtelomere sequences. We applied a relatively low mapq filter
617 cutoff of 10 to the diploid mapping. In a second step we mapped the reads also to the
618 maternal and paternal haploid genomes separately. Mapq scores generally increase for
619 the alignments to the haploid genomes. To identify high confidence alignments, we
620 applied a mapq cutoff of 30 to the haploid genome alignments. A read needed to map to
621 the same chr end in both mappings and pass the two mapq cutoffs to be considered
622 correctly assigned. There were different numbers of reads for specific chromosome
623 ends due to the restriction enzyme sometimes cutting very near a telomere. To
624 minimize this, we used different sets of restriction enzymes for both the initial cutting
625 and for the release and combined the data. This allowed mapping of more reads for
626 some chromosome ends.

627

628 **Pangenome based mapping for chromosome assignment of telomeres from** 629 **diverse individuals**

630 We mapped reads to the pangenome to efficiently capture telomere length across the
631 diverse population. A references file of 500kb of subtelomere sequences was
632 assembled from each of the genomes⁴³ in the pangenome. We mapped our reads
633 from 147 individuals to this reference. We filtered for reads that had a minimum of 2kb

634 alignment to the pangenome reference. To compare telomere length across individuals
635 in Fig. 4, we removed acrocentric chromosomes (13p, 14p, 15p, 21p, 22p) and X and Y
636 subtelomeres (XpYp, and Xq Yq) which recombine in the population. We added these
637 back into the analysis for Extended Data Fig. 5.

638

639 **Statistical Analysis**

640 To determine whether HG002 chromosome specific telomere lengths were significantly different
641 from the individual's grand mean telomere length, we used Analysis of the Mean (ANOM).
642 Statistics were calculated using the R package rstatix (v0.7.0) and ANOM (v0.2)
643 (<https://cran.rproject.org/web/packages/rstatix/index.html>).

644

645 **Data Availability**

646 Data generated during the study will be made available in public sequence repository
647 Sequence Read Archive (SRA) <https://www.ncbi.nlm.nih.gov/sra> and is available upon
648 request.

649

650 **Code availability**

651 The python code for TeloBP, TeloNP and TeloPeakCounter is available at
652 <https://github.com/GreiderLab>

653

654

655 **Acknowledgements**

656 We thank Dr. Rachel Green for provision of laboratory space at Johns Hopkins as well
657 as discussions. Drs. Brendan Cormack and Christine Gao and for reviewing the

658 manuscript. Carla Connelly, Julie Brunelle, and Margaret Strong provided experimental
659 and logistical assistance. We thank Dr. Mary Armanios and her lab for help in the early
660 stages of assay development and Dr. Ludmilla Danilova for statistical analysis. This
661 work was supported by NIH grant R35CA209974 to CWG and Johns Hopkins
662 Bloomberg Distinguished Professorship to CWG.

663

664 **Author contributions**

665 These authors contributed to the following aspects of this work. Conceptualization
666 CWG, KK, SS; Data curation, AG, KK, RK, RWK, AR; Formal analysis, KK, RK, AR;
667 Funding acquisition CWG, HL; Investigation AG, VH, KK, RWK, Methodology, CWG,
668 VH, KK, RK, RWK, AR, SS; Project administration CWG; Resources JA, CWG, JFM,
669 KK; Software KK, RK, HL, AR, K-TT; Supervision CWG, HL; Validation CWG, AG, KK,
670 RK, AR; Visualization JA, KK, RK, AR; Writing original draft CWG, KK Writing – review
671 & editing JA, CWG, AG, VH, KK, AR, SS

672

673 **Competing interest declaration**

674 CWG and KK are inventors of US Patent PCT/US2023/073375 titled "Methods for
675 telomere length measurement".

676

References

- 1 Greider, C. W. & Blackburn, E. H. Identification of a specific telomere terminal transferase activity in *Tetrahymena* extracts. *Cell* **43**, 405-413 (1985).
- 2 Armanios, M. Syndromes of telomere shortening. *Annu Rev Genomics Hum Genet* **10**, 45-61 (2009).
- 3 Armanios, M. The Role of Telomeres in Human Disease. *Annu Rev Genomics Hum Genet* **23**, 363-381 (2022).
- 4 Horn, S. *et al.* TERT promoter mutations in familial and sporadic melanoma. *Science* **339**, 959-961 (2013).
- 5 Huang, F. W. *et al.* Highly recurrent TERT promoter mutations in human melanoma. *Science* **339**, 957-959 (2013).
- 6 Marcand, S., Gilson, E. & Shore, D. A protein-counting mechanism for telomere length regulation in yeast. *Science* **275**, 986-990 (1997).
- 7 Smogorzewska, A. *et al.* Control of human telomere length by TRF1 and TRF2. *Mol Cell Biol* **20**, 1659-1668 (2000).
- 8 Teixeira, M. T., Arneric, M., Sperisen, P. & Lingner, J. Telomere length homeostasis is achieved via a switch between telomerase- extendible and -nonextendible states. *Cell* **117**, 323-335 (2004).

- 9 Blackburn, E. H. & Chiou, S. S. Non-nucleosomal packaging of a tandemly repeated DNA sequence at termini of extrachromosomal DNA coding for rRNA in *Tetrahymena*. *Proc Natl Acad Sci U S A* **78**, 2263-2267 (1981).
- 10 Szostak, J. W. & Blackburn, E. H. Cloning yeast telomeres on linear plasmid vectors. *Cell* **29**, 245-255 (1982).
- 11 Aviv, A. *et al.* Impartial comparative analysis of measurement of leukocyte telomere length/DNA content by Southern blots and qPCR. *Nucleic acids research* **39**, e134 (2011).
- 12 Marcand, S., Wotton, D., Gilson, E. & Shore, D. Rap1p and telomere length regulation in yeast. *Ciba Found Symp* **211**, 76-93; discussion 93-103 (1997).
- 13 Wotton, D. & Shore, D. A novel Rap1p-interacting factor, Rif2p, cooperates with Rif1p to regulate telomere length in *Saccharomyces cerevisiae*. *Genes Dev* **11**, 748-760 (1997).
- 14 Levy, D. L. & Blackburn, E. H. Counting of Rif1p and Rif2p on *Saccharomyces cerevisiae* telomeres regulates telomere length. *Molecular and cellular biology* **24**, 10857-10867 (2004).
- 15 Rufer, N., Dragowska, W., Thornbury, G., Roosnek, E. & Lansdorp, P. M. Telomere length dynamics in human lymphocyte subpopulations measured by flow cytometry [see comments]. *Nat Biotechnol* **16**, 743-747 (1998).
- 16 Aubert, G., Hills, M. & Lansdorp, P. M. Telomere length measurement-caveats and a critical assessment of the available technologies and tools. *Mutation research* **730**, 59-67 (2012).
- 17 Alder, J. K. *et al.* Diagnostic utility of telomere length testing in a hospital-based setting. *Proc Natl Acad Sci U S A* **115**, E2358-E2365 (2018).
- 18 Armanios, M. Telomeres and age-related disease: how telomere biology informs clinical paradigms. *J Clin Invest* **123**, 996-1002 (2013).
- 19 Lansdorp, P. M. *et al.* Heterogeneity in telomere length of human chromosomes. *Hum Mol Genet* **5**, 685-691 (1996).
- 20 Zijlmans, J. M. *et al.* Telomeres in the mouse have large inter-chromosomal variations in the number of T2AG3 repeats. *Proc Natl Acad Sci U S A* **94**, 7423-7428 (1997).
- 21 Martens, U. M. *et al.* Short telomeres on human chromosome 17p. *Nat Genet* **18**, 76-80 (1998).
- 22 Londono-Vallejo, J. A., DerSarkissian, H., Cazes, L. & Thomas, G. Differences in telomere length between homologous chromosomes in humans. *Nucleic Acids Res* **29**, 3164-3171 (2001).
- 23 Sholes, S. L. *et al.* Chromosome-specific telomere lengths and the minimal functional telomere revealed by nanopore sequencing. *Genome Res* **32**, 616-628 (2022).
- 24 Grigorev, K. *et al.* Haplotype diversity and sequence heterogeneity of human telomeres. *Genome Res* (2021).
- 25 Tham, C. Y. *et al.* High-throughput telomere length measurement at nucleotide resolution using the PacBio high fidelity sequencing platform. *Nat Commun* **14**, 281 (2023).
- 26 Dubocanin, D. & Stergachis, A. B. Single-molecule architecture and heterogeneity of human telomeric DNA and chromatin. *BioRxiv* (2022).
- 27 Tan, K. T., Slevin, M. K., Meyerson, M. & Li, H. Identifying and correcting repeat-calling errors in nanopore sequencing of telomeres. *Genome Biol* **23**, 180 (2022).
- 28 Harley, C. B., Futcher, A. B. & Greider, C. W. Telomeres shorten during ageing of human fibroblasts. *Nature* **345**, 458-460 (1990).
- 29 Hastie, N. D. *et al.* Telomere reduction in human colorectal carcinoma and with ageing. *Nature* **346**, 866-868 (1990).
- 30 Vaziri, H. *et al.* Loss of telomeric DNA during aging of normal and trisomy 21 human lymphocytes. *Am. J. Hum. Genet* **52**, 661-667 (1993).

- 31 Aubert, G., Baerlocher, G. M., Vulto, I., Poon, S. S. & Lansdorp, P. M. Collapse of telomere homeostasis in hematopoietic cells caused by heterozygous mutations in telomerase genes. *PLoS Genet* **8**, e1002696 (2012).
- 32 Rufer, N. *et al.* Telomere fluorescence measurements in granulocytes and T lymphocyte subsets point to a high turnover of hematopoietic stem cells and memory T cells in early childhood. *J Exp Med* **190**, 157-167 (1999).
- 33 Martens, U. M. *et al.* Telomere maintenance in human B lymphocytes. *Br J Haematol* **119**, 810-818 (2002).
- 34 Armanios, M. Y. *et al.* Telomerase mutations in families with idiopathic pulmonary fibrosis. *N Engl J Med* **356**, 1317-1326 (2007).
- 35 Van Ziffle, J. A., Baerlocher, G. M. & Lansdorp, P. M. Telomere length in subpopulations of human hematopoietic cells. *Stem Cells* **21**, 654-660 (2003).
- 36 Baerlocher, G. M. & Lansdorp, P. M. Telomere length measurements in leukocyte subsets by automated multicolor flow-FISH. *Cytometry A* **55**, 1-6 (2003).
- 37 Alder, J. K. & Armanios, M. Telomere-mediated lung disease. *Physiol Rev* **102**, 1703-1720 (2022).
- 38 Lakota, K. *et al.* Short lymphocyte, but not granulocyte, telomere length in a subset of patients with systemic sclerosis. *Ann Rheum Dis* **78**, 1142-1144 (2019).
- 39 Garg, S. *et al.* Chromosome-scale, haplotype-resolved assembly of human genomes. *Nat Biotechnol* **39**, 309-312 (2021).
- 40 Stong, N. *et al.* Subtelomeric CTCF and cohesin binding site organization using improved subtelomere assemblies and a novel annotation pipeline. *Genome Res* **24**, 1039-1050 (2014).
- 41 Li, H. Minimap2: pairwise alignment for nucleotide sequences. *Bioinformatics* **34**, 3094-3100 (2018).
- 42 Li, H. New strategies to improve minimap2 alignment accuracy. *Bioinformatics* **37**, 4572-4574 (2021).
- 43 Liao, W. W. *et al.* A draft human pangenome reference. *Nature* **617**, 312-324 (2023).
- 44 Antonarakis, S. E. Short arms of human acrocentric chromosomes and the completion of the human genome sequence. *Genome Res* **32**, 599-607 (2022).
- 45 Graakjaer, J. *et al.* The relative lengths of individual telomeres are defined in the zygote and strictly maintained during life. *Aging Cell* **3**, 97-102 (2004).
- 46 Hemann, M. T., Strong, M. A., Hao, L.-Y. & Greider, C. W. The Shortest Telomere, Not Average Telomere Length, Is Critical for Cell Viability and Chromosome Stability. *Cell* **107**, 67-77 (2001).
- 47 d'Adda di Fagagna, F. *et al.* A DNA damage checkpoint response in telomere-initiated senescence. *Nature* **426**, 194-198 (2003).
- 48 Enomoto, S., Glowczewski, L. & Berman, J. MEC3, MEC1, and DDC2 are essential components of a telomere checkpoint pathway required for cell cycle arrest during senescence in *Saccharomyces cerevisiae*. *Mol Biol Cell* **13**, 2626-2638 (2002).
- 49 Ijpm, A. & Greider, C. W. Short telomeres induce a DNA damage response in *Saccharomyces cerevisiae*. *Mol Biol Cell* **14**, 987-1001 (2003).
- 50 McNally, E. J., Luncsford, P. J. & Armanios, M. Long telomeres and cancer risk: the price of cellular immortality. *J Clin Invest* **130**, 3474-3481 (2019).
- 51 Smogorzewska, A. & de Lange, T. Regulation of telomerase by telomeric proteins. *Annu Rev Biochem* **73**, 177-208 (2004).
- 52 Shore, D. & Bianchi, A. Telomere length regulation: coupling DNA end processing to feedback regulation of telomerase. *Embo J* **28**, 2309-2322 (2009).
- 53 Lustig, A. J. Clues to catastrophic telomere loss in mammals from yeast telomere rapid deletion. *Nat Rev Genet* **4**, 916-923 (2003).

- 54 Zimmermann, M., Kibe, T., Kabir, S. & de Lange, T. TRF1 negotiates TTAGGG repeat-associated replication problems by recruiting the BLM helicase and the TPP1/POT1 repressor of ATR signaling. *Genes Dev* **28**, 2477-2491 (2014).
- 55 Paschini, M. *et al.* Spontaneous replication fork collapse regulates telomere length homeostasis in wild type cells. *bioRxiv* (2020).
- 56 Arneric, M. & Lingner, J. Tel1 kinase and subtelomere-bound Tbf1 mediate preferential elongation of short telomeres by telomerase in yeast. *EMBO reports* **8**, 1080-1085 (2007).
- 57 Brown, W. R. A. *et al.* Structure and polymorphism of human telomere-associated DNA. *Cell* **63**, 119-132 (1990).
- 58 Nergadze, S. G. *et al.* CpG-island promoters drive transcription of human telomeres. *RNA* **15**, 2186-2194 (2009).
- 59 Deng, Z. *et al.* A role for CTCF and cohesin in subtelomere chromatin organization, TERRA transcription, and telomere end protection. *Embo J* **31**, 4165-4178 (2012).
- 60 Feretzaki, M., Renck Nunes, P. & Lingner, J. Expression and differential regulation of human TERRA at several chromosome ends. *RNA* **25**, 1470-1480 (2019).
- 61 Achrem, M., Szucko, I. & Kalinka, A. The epigenetic regulation of centromeres and telomeres in plants and animals. *Comp Cytogenet* **14**, 265-311 (2020).
- 62 Toubiana, S. & Selig, S. Human subtelomeric DNA methylation: regulation and roles in telomere function. *Curr Opin Genet Dev* **60**, 9-16 (2020).
- 63 Gonzalo, S. *et al.* DNA methyltransferases control telomere length and telomere recombination in mammalian cells. *Nat Cell Biol* **8**, 416-424 (2006).
- 64 Arnoult, N. *et al.* Replication timing of human telomeres is chromosome arm-specific, influenced by subtelomeric structures and connected to nuclear localization. *PLoS Genet* **6**, e1000920 (2010).
- 65 Armanios, M. & Blackburn, E. H. The telomere syndromes. *Nat Rev Genet* **13**, 693-704 (2012).
- 66 Hao, L. Y. *et al.* Short telomeres, even in the presence of telomerase, limit tissue renewal capacity. *Cell* **123**, 1121-1131 (2005).
- 67 Slagboom, P. E., Droog, S. & Boomsma, D. I. Genetic determination of telomere size in humans: a twin study of three age groups. *Am J Hum Genet* **55**, 876-882 (1994).
- 68 Conklin, Q. A., Crosswell, A. D., Saron, C. D. & Epel, E. S. Meditation, stress processes, and telomere biology. *Curr Opin Psychol* **28**, 92-101 (2019).
- 69 Greider, C. W. Telomeres, telomerase and senescence. *Bioessays* **12**, 363-369 (1990).
- 70 de Lange, T. *et al.* Structure and variability of human chromosome ends. *Mol. Cell. Biol.* **10**, 518-527 (1990).
- 71 American Thoracic Society. Idiopathic pulmonary fibrosis: diagnosis and treatment. International consensus statement. American Thoracic Society (ATS), and the European Respiratory Society (ERS). *Am J Respir Crit Care Med* **161**, 646-664 (2000).

Figure 1

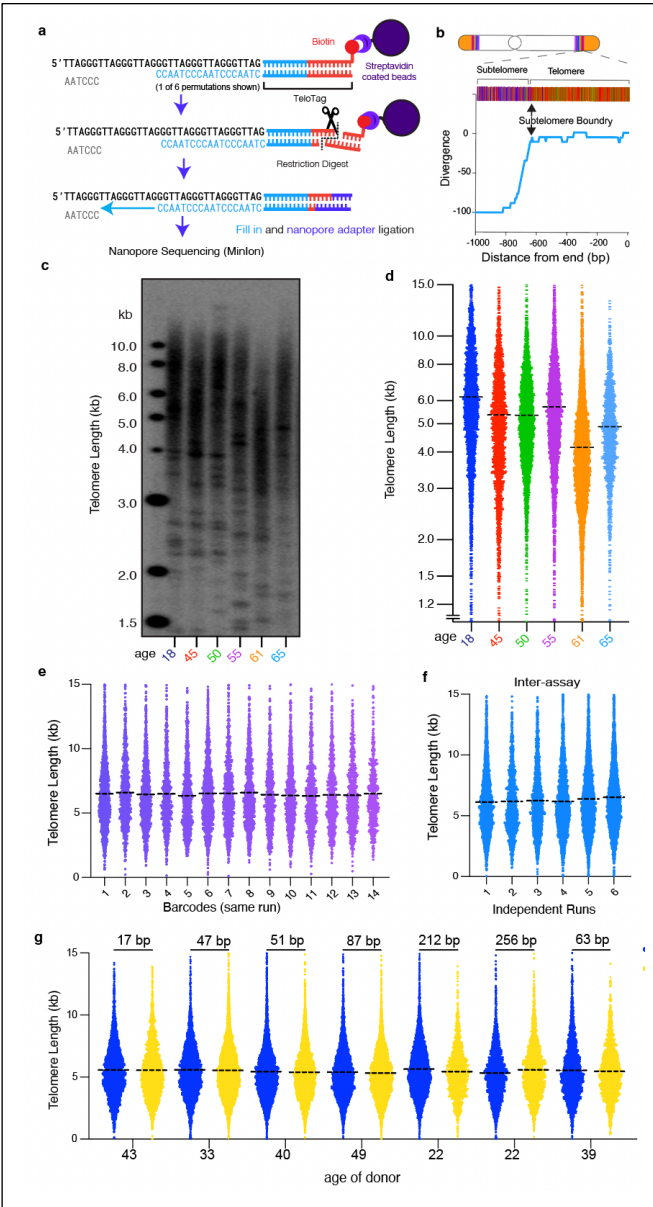


Fig.1 | Nanopore telomere profiling is accurate and precise. **a** Schematic depicting nanopore telomere profiling enrichment strategy. Telomeres are tagged with a biotin adapter (TeloTag), enriched by streptavidin pull down, and sequenced. **b** Subtelomere boundary is identified using an algorithm that detects significant deviation from the telomere repeat pattern. **c** Southern blot of telomere lengths from 6 individuals. **d** Telomere length measured by Nanopore telomere profiling for the same individuals as in **c**. (total reads = 21,556). The dashed line represents the mean telomere length of each distribution. Each point represents a single telomere read. **e** Inter assay variability. Telomere length from a single donor was measured 14 times on a single flow cell (total reads = 13,256). **f** Inter-assay variability: Telomere length measured from a single donor across 6 flow cells (total reads = 19,230). **g** Telomere length profiles from the same samples generated in two different laboratories JH=Johns Hopkins (blue), SC=UC Santa Cruz (gold). The difference in telomere length in base pairs is shown at the top.

Figure 2

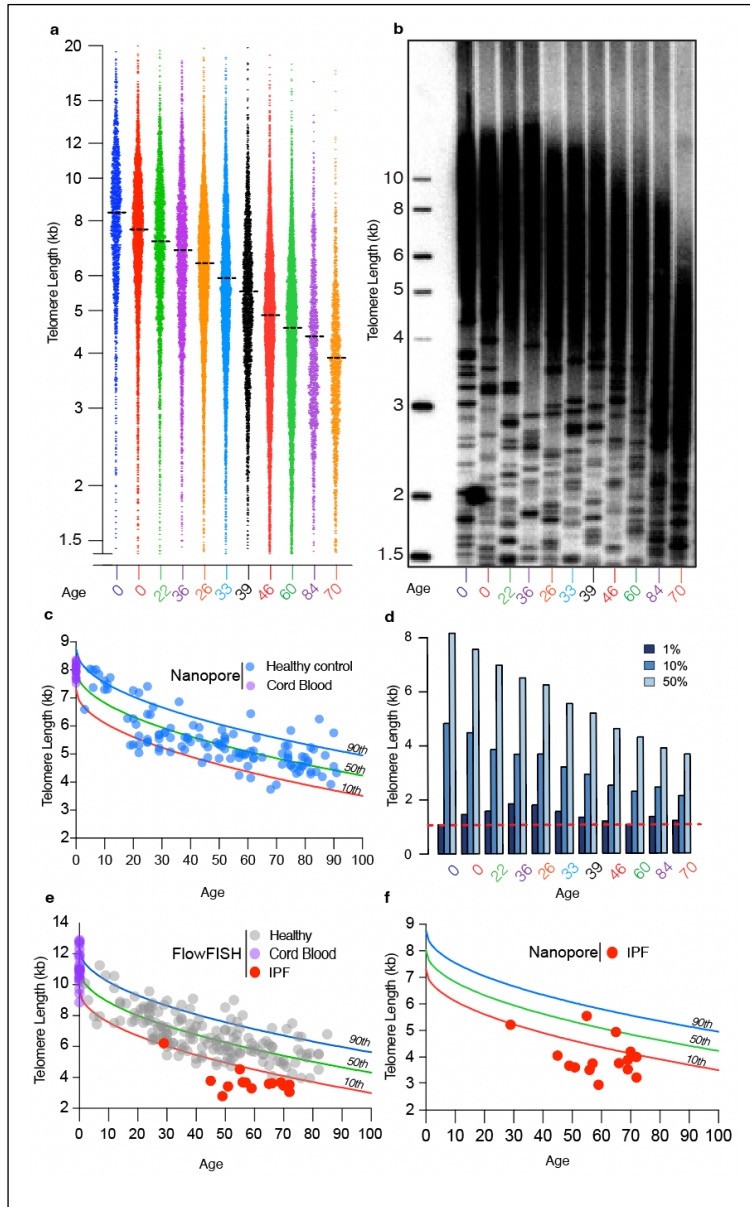


Fig. 2 | Nanopore telomere profiling identified population distribution of telomere shortening with age similar to FlowFISH. a. Nanopore telomere length profiles for 11 samples selected, age is noted at bottom. Each point is an individual read (total reads = 47624) **b.** Southern of same samples as **a.**, Age of individual noted at bottom **c.** The mean telomere length was determined for 132 individuals aged 0 to 91 (blue dots) (total reads = ~920,000). Cord blood lengths are shown in purple. We calculated the population distribution and show confidence intervals for the 90th percentile (blue), the median (green line) and 10th percentiles (red) for telomere length in this population using parameters established previously for FlowFISH¹⁷ **e.** Lymphocyte telomere length from FlowFISH data from Alder et al. (gray dots) and cord blood (purple dots). The lengths for 15 human subjects with IPF (red) were

determined by FlowFISH (Methods) One point represents two individuals who have nearly identical length and are indistinguishable in the figure. **f.** Nanopore telomere length profiles from the same 15 subjects with short telomere syndrome shown in **e.** plotted against population distribution from **c** (total reads = 32457).

Figure 3

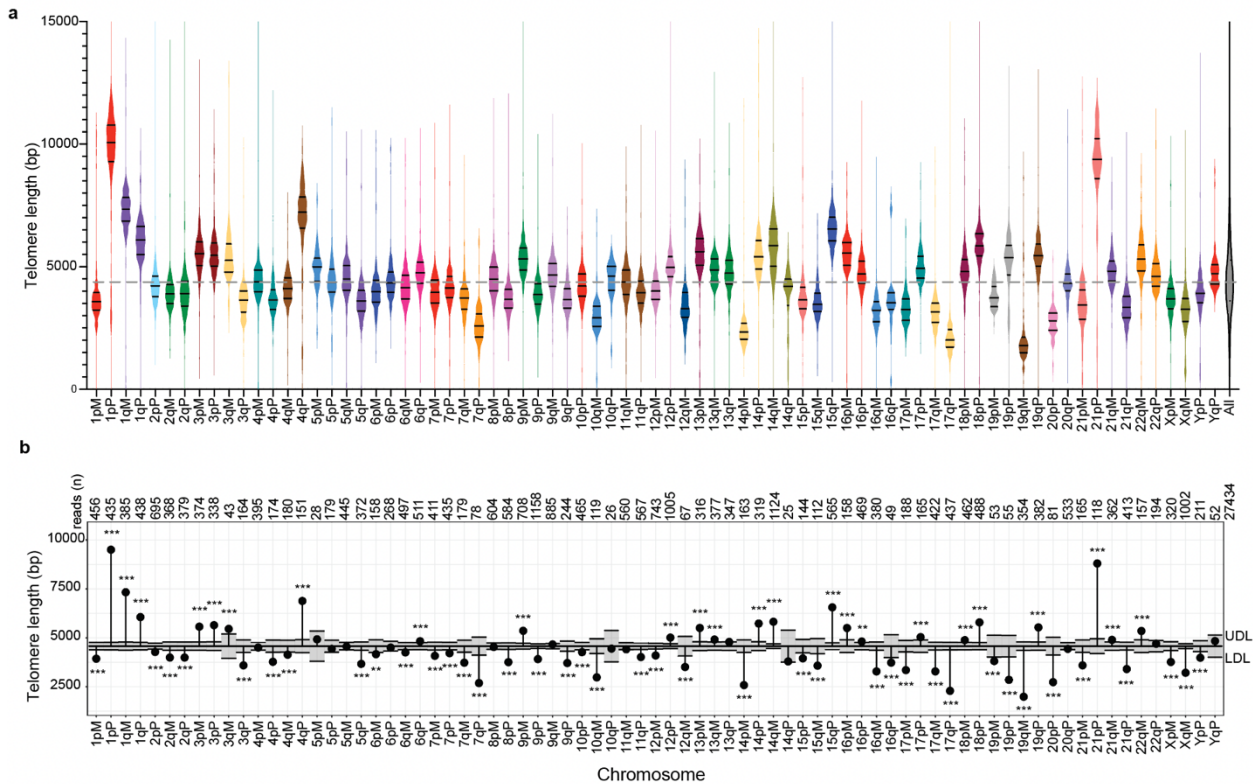


Fig. 3 | Chromosome end-specific telomere lengths **a.** Violin plots of the distribution of telomere lengths for 77 telomeres from HG002 that mapped with confidence and passed our filters (see methods) Total reads $n=27,433$. Each end is labeled with the chromosome number and p for the short and q for long arms. The haplotypes for each chromosome end are labeled Maternal (M) and Paternal (P) and colored with the same colors for allelic pairs. The mean, 90th and 10th percentile for each distribution are shown with short horizontal black lines in each violin plot. The distribution of all telomeres lengths across all chromosomes ends is at the far right (All). The dashed line represents the grand mean of all telomeres **b.** Analysis of the means (ANOM) multiple contrast test of each telomere length distribution against the grand mean of all telomere lengths for data in **a.** The number of reads for each chromosome end is shown at the top. P-values were adjusted for multiple hypotheses testing using the Bonferroni method. Chromosome ends with length profiles reaching outside of the shaded gray region between the upper decision limit (UDL) and lower decision limit (LDL) are considered significantly different from the grand mean. (*), $p \leq 0.05$, (**), $p \leq 0.01$. (***), $p \leq 0.001$; nonsignificant differences have no stars.

Figure 4

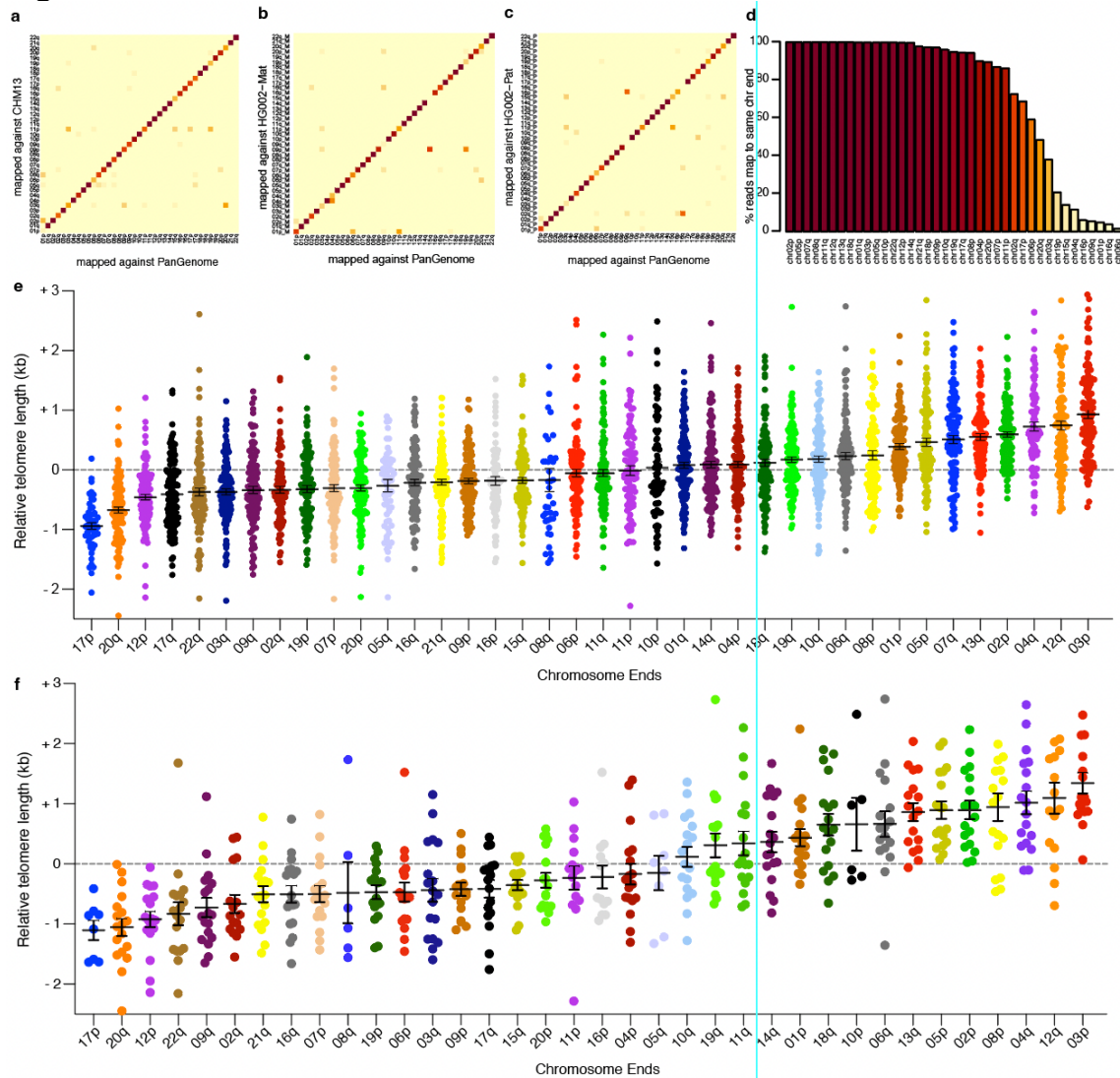


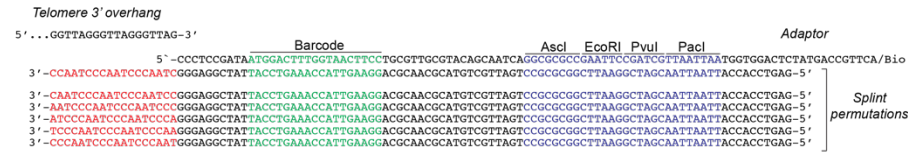
Fig. 4 | Conserved telomere lengths across 147 individuals with reads mapping to the pangenome.

We used the pangenome reference to assign reads to chromosome ends for ~92000 telomere reads obtained from 147 individuals. **a.** Matrix heatmap shows what fraction of reads that mapped to a given chromosome end in the pangenome (column) and where they map in CHM13 (rows) with a mapq of 60. Light yellow indicates 0% and dark red indicates 100% of reads mapping to the respective CHM13 chromosome end. **b.** As in **a.** but mapping to the HG002 Maternal reference **c.** As in **a.** but mapping reads to the HG002 Paternal reference genome. **d.** Bar graph showing the fraction of reads that mapped for each chromosome end in the pangenome to the same chromosome end in all three haploid genomes (CHM13, HG002 maternal and HG002 paternal). Colors are the same as in the heatmaps **a.**, **b.** and **c.** **e.** To determine the relative telomere length, we calculated grand mean telomere length for a given individual and subtracted it from the chromosome specific mean telomere length for each chromosome end in that individual. Zero indicates no difference between the specific chromosome end mean telomere length and the individual's grand mean telomere length. Bars represent mean length of a given telomere in all individuals and whiskers represent the standard error of the mean. **f.** Same as in **e.** but for cord blood samples only.

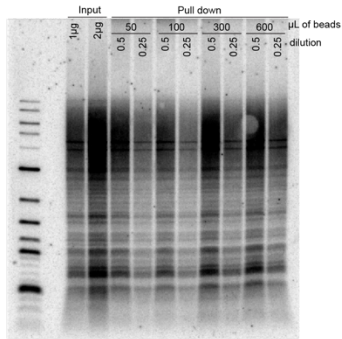
Extended Data Figures

Extended Data Fig 1

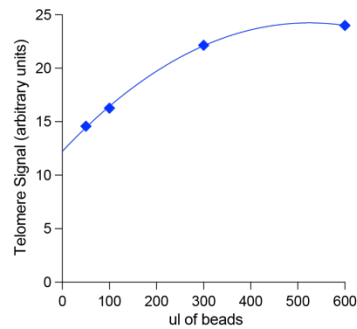
a



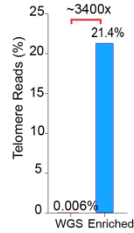
b



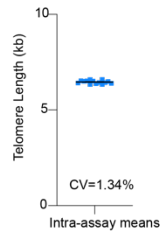
c



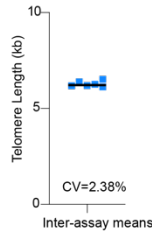
d



e



f

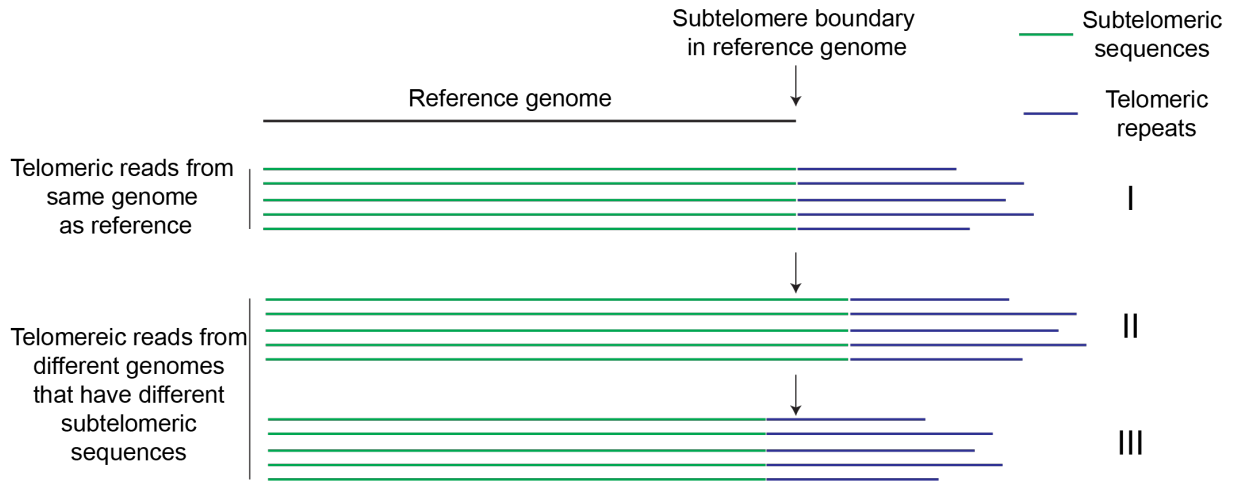


Extended Data Fig. 1. Quantitation of enrichment and assay reproducibility. a.

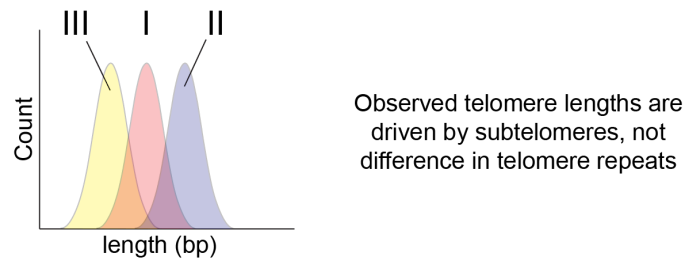
Sequence of one representative TeloTag adaptor. The barcoded adaptor (top strand) is annealed to a mixture of splints that have all 6 permutations of the CCCTAA sequence to improve chances of in-frame annealing to the telomere 3' overhang. **b.** Southern blot of telomeres recovered after biotin pull down using different volumes of streptavidin bead enrichment. **c.** Quantification of the efficiency of enrichment using increasing ratio of streptavidin beads to DNA. **d.** Enrichment of telomeric reads using biotin pull down relative to WGS. **e.** Intra-assay coefficient of variation (CV) of one single with different barcodes measured multiple times on the same flow cell. **f.** Inter-assay coefficient of variation (CV) of one sample measured multiple times across different flow cells. Mean telomere length of a single sample measured on multiple different runs.

Extended Data Fig 2

a



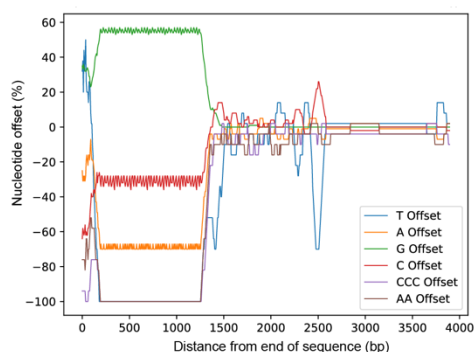
b



Extended Data Fig. 2: Heterogeneity in human subtelomere sequence means the telomere subtelomere boundary point can differ in sequence reads from diverse genomes and the reference genome a. Telomere reads from the DNA identical to the reference genome will align at the boundary point in the reference. However, for some individuals a telomeric read will map well but there is extra sequence past the reference boundary point. For others there may be less subtelomere sequence on the read b. When telomere length is determined by mapping to the reference sequence boundary point, this can lead to incorrectly longer (II) or incorrectly shorter (III) telomere length distributions.

Extended Data Fig 3

a



b

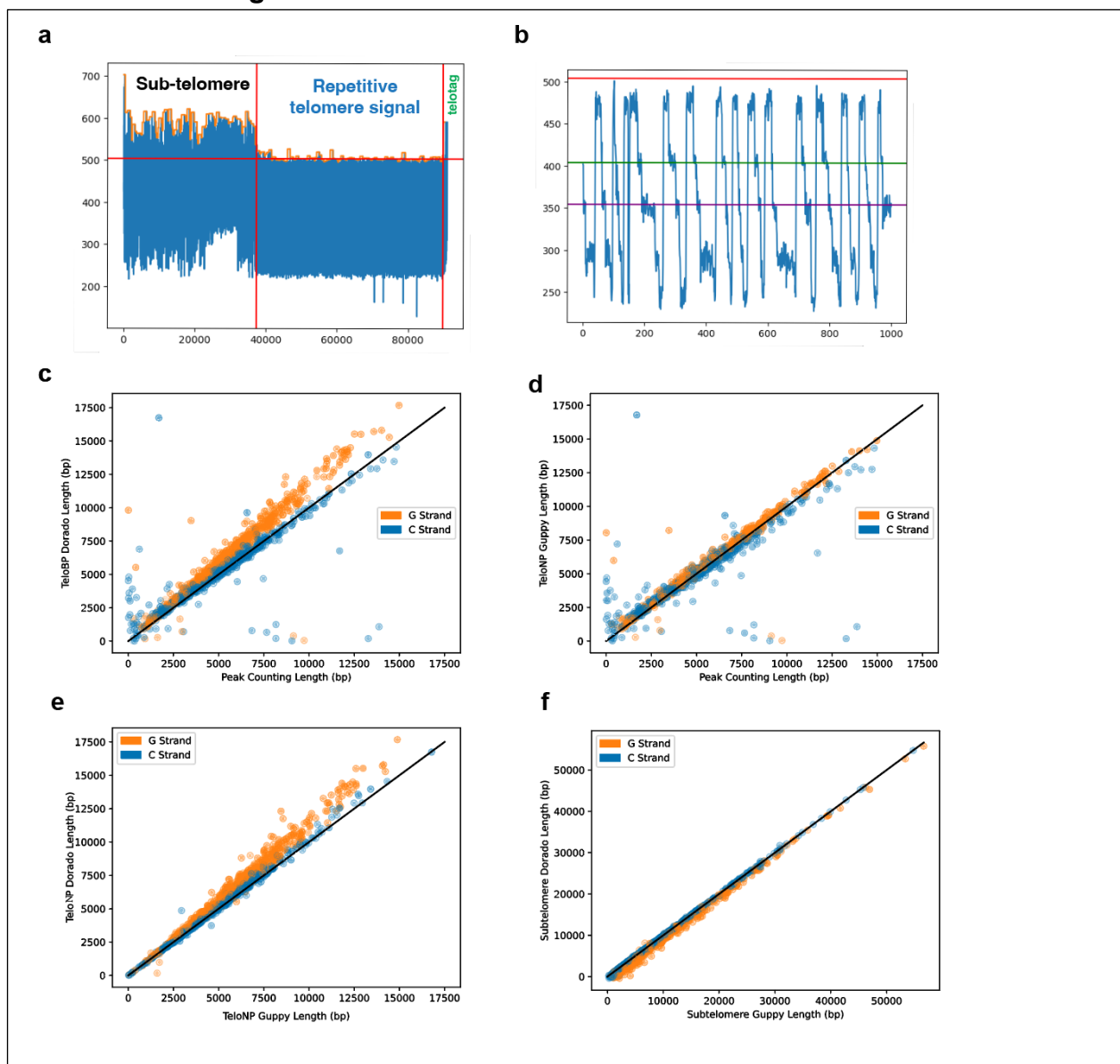


c



Extended Data Fig. 3: Establishing telomere boundary points with TeloBP algorithm **a.** Representation of the nucleotide offsets for several different parameters as a rolling window scanning from telomere end on right (see methods). **b.** IGV view of the telomere sequence and where the boundary is called **c.** Example of where TeloBP incorporates variant repeats into the telomere, compared to method setting a boundary of 4 consecutive repeats of TTAGGG.

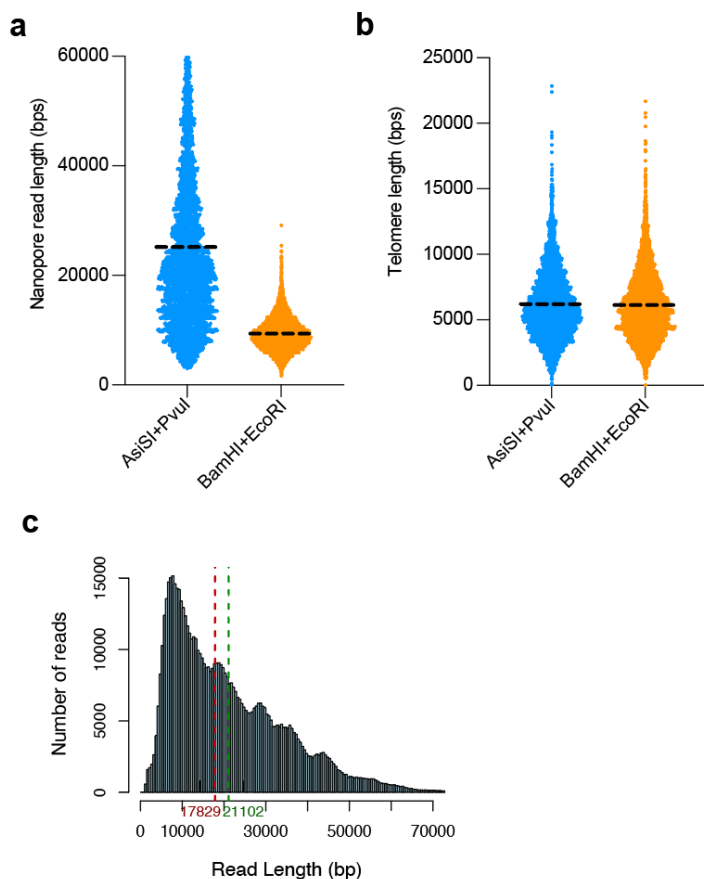
Extended Data Fig 4



Extended Data Fig 4: Analysis of telomere length by TeloPeakCounter. a.

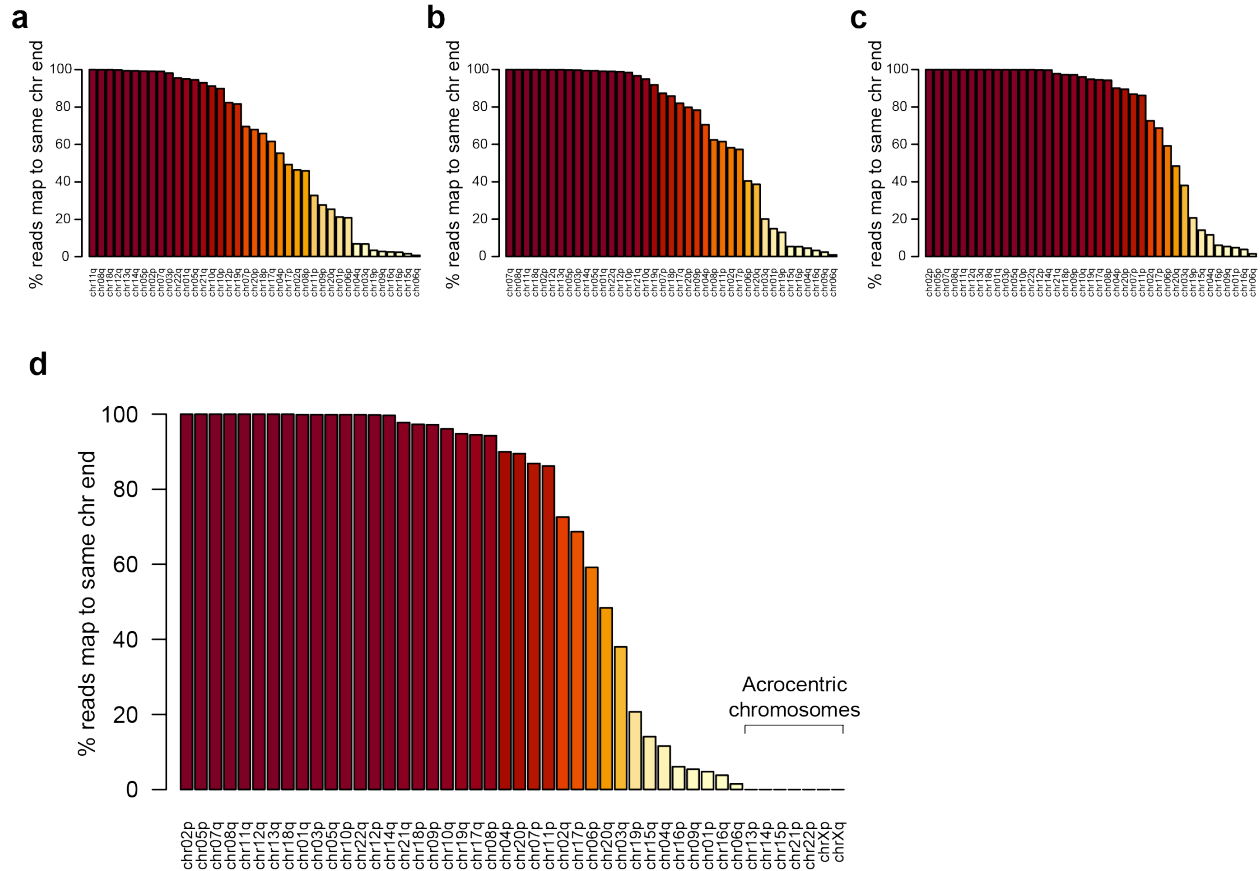
Representation of the subtelomere and telomere sequence electrical signal **b**. High resolution image of peaks in the telomere repeats in electrical signal. Comparison of Guppy (version 6.5.7+ca6d6af) versus Dorado (version 0.3.1) base caller. Each blue dot represents an individual telomere read. 2435 read were examined from one data set (F63) from Fig 2. **c**. Comparison of telomere length determined by the peak counting vs Dorado base calling Blue dots represent C-strand reads, orange dots represent G-Strand reads. **d**. Comparison of telomere length determined by the peak counting vs Guppy base calling. **e**. Comparison of Guppy telomere length by TeloNP vs Dorado. **f**. Comparison of subtelomere length with Guppy vs Dorado.

Extended Data Fig 5



Extended Data Fig 5. Length of fragments does not affect telomere length determination. **a.** The length of the fragments when genomic DNA is cut with AsiSI and PvuI is shown in blue. The length of the fragments when cut with BamHI and EcoRI is shown in orange. **b.** The telomere length of fragments cut with AsiSI and PvuI is in blue and BamHI and EcoRI is shown in orange. **c.** The distribution of fragment lengths for 640,000 reads that mapped to pangenome with 1kb alignment reads: the Y axis is the number of reads and the X axis is the length in base pairs. The red dashed line is the median and the green dashed line is the mean length.

Extended Data Fig 6



Extended Data Fig. 6. Concordance of reads mapped to the pangenome with mapping to CHM13 and HG002 Mat and HG002 Pat. We used different mapq scores to quantitate the fraction of reads that mapped to the same chromosome ends as the pangenome and the three referenced genomes **a.** Mapq score of 1 **b.** Mapq score of 30 **c.** Mapq score of 60. **d.** In previous analysis the acrocentric were omitted. Here they were included 13p,14p,15p, 21p and 22p and show less than 1% of reads mapped to the same chromosome ends for these acrocentric.

Extended Data Table 1. Samples included in comparison of FlowFISH and Telomere Profiling

<i>Sample</i>	<i>age</i>	<i>FlowFISH lymphocyte length (bps)</i>	<i>FlowFISH granulocyte length (bps)</i>	<i>Telomere profiling length (bps)</i>
1	29	6210	5480	5045
2	45	3790	3860	4054
3	49	2790	3640	3678
4	51	3420	4020	3609
5	55	4520	4860	5545
6	56	3690	3990	3519
7	57	3670	2830	3759
8	59	3300	3600	2954
9	65	3580	4250	4945
10	66	3630	4430	3774
11	69	3670	3990	3541
12	69	3670	4300	3883
13	70	3480	4500	4203
14	72	3060	3090	3236
15	72	3530	4000	4003

Extended Data Table 2 Oligonucleotides in this study

NB50_Indi_AscI_EcoRI_PvuI-HF_Pacl	/5Phos/CCCTCCGATAATGGACTTTGGTAACTTCTGCGTTGCGTACAGCAATCAGGCGCGCCGAATTCGATCGTTAATTAATGGTGGACTCTATGACCGTTCA/3BioTEG/
NB50.C1	GAGTCCACCATTAATTAACGATCGGAATTCGGCGCGCCTGATTGCTGTACGCAACGCAGGAAGTTACCAAAGTCCATTATCGGAGGGACCCCTAACCCCTAACCCCTA
NB50.C2	GAGTCCACCATTAATTAACGATCGGAATTCGGCGCGCCTGATTGCTGTACGCAACGCAGGAAGTTACCAAAGTCCATTATCGGAGGGACCCCTAACCCCTAACCCCT
NB50.C3	GAGTCCACCATTAATTAACGATCGGAATTCGGCGCGCCTGATTGCTGTACGCAACGCAGGAAGTTACCAAAGTCCATTATCGGAGGGTAACCCCTAACCCCTAACCC
NB50.C4	GAGTCCACCATTAATTAACGATCGGAATTCGGCGCGCCTGATTGCTGTACGCAACGCAGGAAGTTACCAAAGTCCATTATCGGAGGGCTAACCCCTAACCCCTAACCC
NB50.C5	GAGTCCACCATTAATTAACGATCGGAATTCGGCGCGCCTGATTGCTGTACGCAACGCAGGAAGTTACCAAAGTCCATTATCGGAGGGCTAACCCCTAACCCCTAAC
NB50.C6	GAGTCCACCATTAATTAACGATCGGAATTCGGCGCGCCTGATTGCTGTACGCAACGCAGGAAGTTACCAAAGTCCATTATCGGAGGGCCCTAACCCCTAACCCCTAA
NB65_Indi_AscI_EcoRI_PvuI-HF_Pacl	/5Phos/CCCTCCGATATTCTCAGTCTTCTCCAGACAAGGTGCGTACAGCAATCAGGCGCGCCGAATTCGATCGTTAATTAATGGTGGACTCTATGACCGTTCA/3BioTEG/
NB65.C1	GAGTCCACCATTAATTAACGATCGGAATTCGGCGCGCCTGATTGCTGTACGCACCTTGCTGGAGGAAGACTGAGAATATCGGAGGGACCCCTAACCCCTAACCCCTA
NB65.C2	GAGTCCACCATTAATTAACGATCGGAATTCGGCGCGCCTGATTGCTGTACGCACCTTGCTGGAGGAAGACTGAGAATATCGGAGGGACCCCTAACCCCTAACCCCT
NB65.C3	GAGTCCACCATTAATTAACGATCGGAATTCGGCGCGCCTGATTGCTGTACGCACCTTGCTGGAGGAAGACTGAGAATATCGGAGGGTAACCCCTAACCCCTAACCC
NB65.C4	GAGTCCACCATTAATTAACGATCGGAATTCGGCGCGCCTGATTGCTGTACGCACCTTGCTGGAGGAAGACTGAGAATATCGGAGGGCTAACCCCTAACCCCTAACCC
NB65.C5	GAGTCCACCATTAATTAACGATCGGAATTCGGCGCGCCTGATTGCTGTACGCACCTTGCTGGAGGAAGACTGAGAATATCGGAGGGCTAACCCCTAACCCCTAAC
NB65.C6	GAGTCCACCATTAATTAACGATCGGAATTCGGCGCGCCTGATTGCTGTACGCACCTTGCTGGAGGAAGACTGAGAATATCGGAGGGCCCTAACCCCTAACCCCTAA
NB68_Indi_AscI_EcoRI_PvuI-HF_Pacl	/5Phos/CCCTCCGATAGAATCTAAGCAAACACGAAGGTGCGTACAGCAATCAGGCGCGCCGAATTCGATCGTTAATTAATGGTGGACTCTATGACCGTTCA/3BioTEG/
NB68.C1	GAGTCCACCATTAATTAACGATCGGAATTCGGCGCGCCTGATTGCTGTACGCACCCCTGGTGTGGCTTAGATTCTATCGGAGGGACCCCTAACCCCTAACCCCTA
NB68.C2	GAGTCCACCATTAATTAACGATCGGAATTCGGCGCGCCTGATTGCTGTACGCACCCCTGGTGTGGCTTAGATTCTATCGGAGGGACCCCTAACCCCTAACCCCT
NB68.C3	GAGTCCACCATTAATTAACGATCGGAATTCGGCGCGCCTGATTGCTGTACGCACCCCTGGTGTGGCTTAGATTCTATCGGAGGGTAACCCCTAACCCCTAACCC
NB68.C4	GAGTCCACCATTAATTAACGATCGGAATTCGGCGCGCCTGATTGCTGTACGCACCCCTGGTGTGGCTTAGATTCTATCGGAGGGCTAACCCCTAACCCCTAACCC
NB68.C5	GAGTCCACCATTAATTAACGATCGGAATTCGGCGCGCCTGATTGCTGTACGCACCCCTGGTGTGGCTTAGATTCTATCGGAGGGCTAACCCCTAACCCCTAAC
NB68.C6	GAGTCCACCATTAATTAACGATCGGAATTCGGCGCGCCTGATTGCTGTACGCACCCCTGGTGTGGCTTAGATTCTATCGGAGGGCCCTAACCCCTAACCCCTAA
NB88_Indi_AscI_EcoRI_PvuI-HF_Pacl	/5Phos/CCCTCCGATATCTTACTACCGATCCGAAGCAGTGCCTACAGCAATCAGGCGCGCCGAATTCGATCGTTAATTAATGGTGGACTCTATGACCGTTCA/3BioTEG/
NB88.C1	GAGTCCACCATTAATTAACGATCGGAATTCGGCGCGCCTGATTGCTGTACGCACTGCTTCGGATCGGTAGTAGAAGATATCGGAGGGACCCCTAACCCCTAACCCCTA
NB88.C2	GAGTCCACCATTAATTAACGATCGGAATTCGGCGCGCCTGATTGCTGTACGCACTGCTTCGGATCGGTAGTAGAAGATATCGGAGGGACCCCTAACCCCTAACCCCT
NB88.C3	GAGTCCACCATTAATTAACGATCGGAATTCGGCGCGCCTGATTGCTGTACGCACTGCTTCGGATCGGTAGTAGAAGATATCGGAGGGTAACCCCTAACCCCTAACCC
NB88.C4	GAGTCCACCATTAATTAACGATCGGAATTCGGCGCGCCTGATTGCTGTACGCACTGCTTCGGATCGGTAGTAGAAGATATCGGAGGGCTAACCCCTAACCCCTAACCC
NB88.C5	GAGTCCACCATTAATTAACGATCGGAATTCGGCGCGCCTGATTGCTGTACGCACTGCTTCGGATCGGTAGTAGAAGATATCGGAGGGCTAACCCCTAACCCCTAAC
NB88.C6	GAGTCCACCATTAATTAACGATCGGAATTCGGCGCGCCTGATTGCTGTACGCACTGCTTCGGATCGGTAGTAGAAGATATCGGAGGGCCCTAACCCCTAACCCCTAA
NB01-Phos_AscI_PvuI-HF_EcoRI_Pacl	/5Phos/CCCTCCGATACACAAAGACCCGACAACCTTTCTTTCGCTACAGCAATCAGGCGCGCCGATCGGAATTCCTAATTAATGGTGGACTCTATGACCGTTCA/3BioTEG/
N01.C1	GAGTCCACCATTAATTAACCTAAGGCTAGCGGCGCGCCTGATTGCTGTACGCAAGAAAGTTGTCGGTGTCTTTGTGTATCGGAGGGACCCCTAACCCCTAACCCCTA
N01.C2	GAGTCCACCATTAATTAACCTAAGGCTAGCGGCGCGCCTGATTGCTGTACGCAAGAAAGTTGTCGGTGTCTTTGTGTATCGGAGGGACCCCTAACCCCTAACCCCT
N01.C3	GAGTCCACCATTAATTAACCTAAGGCTAGCGGCGCGCCTGATTGCTGTACGCAAGAAAGTTGTCGGTGTCTTTGTGTATCGGAGGGTAACCCCTAACCCCTAACCC
N01.C3	GAGTCCACCATTAATTAACCTAAGGCTAGCGGCGCGCCTGATTGCTGTACGCAAGAAAGTTGTCGGTGTCTTTGTGTATCGGAGGGCTAACCCCTAACCCCTAACCC
N01.C4	GAGTCCACCATTAATTAACCTAAGGCTAGCGGCGCGCCTGATTGCTGTACGCAAGAAAGTTGTCGGTGTCTTTGTGTATCGGAGGGCTAACCCCTAACCCCTAAC

N01.C5	GAGTCCACCATTAATTAACCTAAGGCTAGCGGCGCGCCTGATTGCTGTACGCAAAGAAAGTTGTCGGTGTCTTTGTGTATCGGAGGGCCCTAACCCCTAACCCCTAA
NB70-Phos_AscI_PvuII-HF_EcoRI_PacI	/5Phos/CCCTCCGATAACCGAGATCCTACGAATGGAGTGTTCGCTACAGCAATCAGGCGCGCCCGATCGGAATTCTTAATTAATGGTGGACTCTATGACCGTTCA/3BioTEG/
NB70.C1	GAGTCCACCATTAATTAACCTAAGGCTAGCGGCGCGCCTGATTGCTGTACGCAAACTCCATTCTAGGATCTCGGTTATCGGAGGGACCCTAACCCCTAACCCCTA
NB70.C2	GAGTCCACCATTAATTAACCTAAGGCTAGCGGCGCGCCTGATTGCTGTACGCAAACTCCATTCTAGGATCTCGGTTATCGGAGGGAAACCCTAACCCCTAACCCCT
NB70.C3	GAGTCCACCATTAATTAACCTAAGGCTAGCGGCGCGCCTGATTGCTGTACGCAAACTCCATTCTAGGATCTCGGTTATCGGAGGGTAACCCTAACCCCTAACCCCT
NB70.C4	GAGTCCACCATTAATTAACCTAAGGCTAGCGGCGCGCCTGATTGCTGTACGCAAACTCCATTCTAGGATCTCGGTTATCGGAGGGCTAACCCCTAACCCCTAACCC
NB70.C5	GAGTCCACCATTAATTAACCTAAGGCTAGCGGCGCGCCTGATTGCTGTACGCAAACTCCATTCTAGGATCTCGGTTATCGGAGGGCTAACCCCTAACCCCTAACCC
NB70.C6	GAGTCCACCATTAATTAACCTAAGGCTAGCGGCGCGCCTGATTGCTGTACGCAAACTCCATTCTAGGATCTCGGTTATCGGAGGGCCCTAACCCCTAACCCCTAA